



ACADEMIC
PRESS

Available online at www.sciencedirect.com

SCIENCE @ DIRECT®

Molecular Phylogenetics and Evolution 26 (2003) 452–475

MOLECULAR
PHYLOGENETICS
AND
EVOLUTION

www.elsevier.com/locate/ympev

Molecular systematics and phylogeography of Amazonian poison frogs of the genus *Dendrobates*

R. Symula,^a R. Schulte,^b and K. Summers^{a,*}

^a Department of Biology, East Carolina University, Greenville, NC 27858, USA

^b Instituto de Investigación de la Biología de las Cordilleras Orientales, Tarapoto, Peru

Received 2 January 2002; revised 12 July 2002

Abstract

The study of Amazonian biodiversity requires detailed knowledge of the phylogenetic relationships of closely related taxa distributed across Amazonia. The Amazonian poison frogs of the genus *Dendrobates* have undergone many taxonomic revisions, but the phylogenetic relationships within this group remain poorly understood. Most previous classifications were based on morphology and skin toxin analyses, with limited use of DNA sequence data. Using mtDNA sequence data from four gene regions (cytochrome *b*, cytochrome oxidase I, 16S rRNA, and 12S rRNA), we present a molecular phylogenetic analysis of the evolutionary relationships within a representative group of Amazonian *Dendrobates*. We use the resulting phylogenetic hypothesis to investigate different biogeographic hypotheses concerning genetic divergence and species diversity in Amazonia. The results of the analysis support the presence of ancient paleogeographic barriers to gene flow between eastern and western Amazonia, and indicate substantial genetic divergence between species found in the northern and southern regions of western Amazonia.

© 2002 Elsevier Science (USA). All rights reserved.

1. Introduction

The Amazon Basin harbors an inordinate proportion of the world's biodiversity. This immense diversity has delayed progress in determining the phylogenetic relationships among Amazonian organisms. Nevertheless, an understanding of the systematic relationships of Amazonian species plays a critical role in evaluating hypotheses which attempt to explain the high levels of diversity in the region (Patton and da Silva, 1998). Recently, substantial progress has been made via molecular systematic investigation of the phylogenetic and biogeographic relationships within a variety of Amazonian taxa, including amphibians (e.g., Chek et al., 2001), shedding light on important questions concerning Amazonian biodiversity. Here we present a molecular systematic analysis of phylogenetic and biogeographic relationships among populations and species of Ama-

zonian poison frogs of the genus *Dendrobates*, focusing on western Amazonia.

There are a variety of species of *Dendrobates* in Amazonia and this genus forms a substantial part of the family Dendrobatidae (Clough and Summers, 2000; Myers, 1987; Vences et al., 2000). Early descriptions of Amazonian *Dendrobates* included *Dendrobates quinquevittatus* (Fitzinger in Steindachner, 1864), *Dendrobates reticulatus* Boulenger (1883), *Dendrobates fantasticus* Boulenger (1883), *Dendrobates galactonotus* (Fitzinger in Steindachner, 1864) and *Dendrobates ventrimaculatus* Shreve (1935). Most of these species were placed by Silverstone (1975) into a single polymorphic species: "*D. quinquevittatus*." Caldwell and Myers (1990) restricted *D. quinquevittatus* to describe a frog with a distinct color pattern occurring in specific regions of Rondonia and Amazonas, Brazil, and described a new species (*Dendrobates castaneoticus*). They also tentatively assigned a number of widespread populations of Amazonian *Dendrobates* with small body size and similar coloration to the species *D. ventrimaculatus*, but suggested that this species might represent a composite of several species. A variety of other species of

* Corresponding author. Fax: 1-252-328-4178.

E-mail address: summersk@mail.ecu.edu (K. Summers).

Amazonian *Dendrobates* have been described, including *Dendrobates mysteriosus* Myers (1982), *Dendrobates imitator* Schulte (1986), *Dendrobates variabilis* Zimmerman and Zimmerman (1988), *Dendrobates duellmani* Schulte (1999), *Dendrobates amazonicus* Schulte (1999), *Dendrobates flavovittatus* Schulte 1999, *Dendrobates rubrocephalus* Schulte 1999, *D. imitator* Schulte (1986), *Dendrobates sirensis* Aichinger (1991), *Dendrobates lamasi* Morales (1992), and *Dendrobates biolat* Morales (1992). However, not all of these species are generally accepted as valid (see Section 3).

Members of the genus *Dendrobates* are distributed across most of Amazonia, but species diversity is highest in western Amazonia; Figs. 1 and 2). With the exception of *D. galactonotus* and *D. mysteriosus*, Amazonian species of *Dendrobates* are morphologically similar in body size and shape (although frequently divergent in color and pattern). This suggests that these frogs comprise a group of closely related species. However, the evolutionary relationships among these species are poorly understood. Using a molecular phylogenetic approach, we attempt to clarify these relationships.

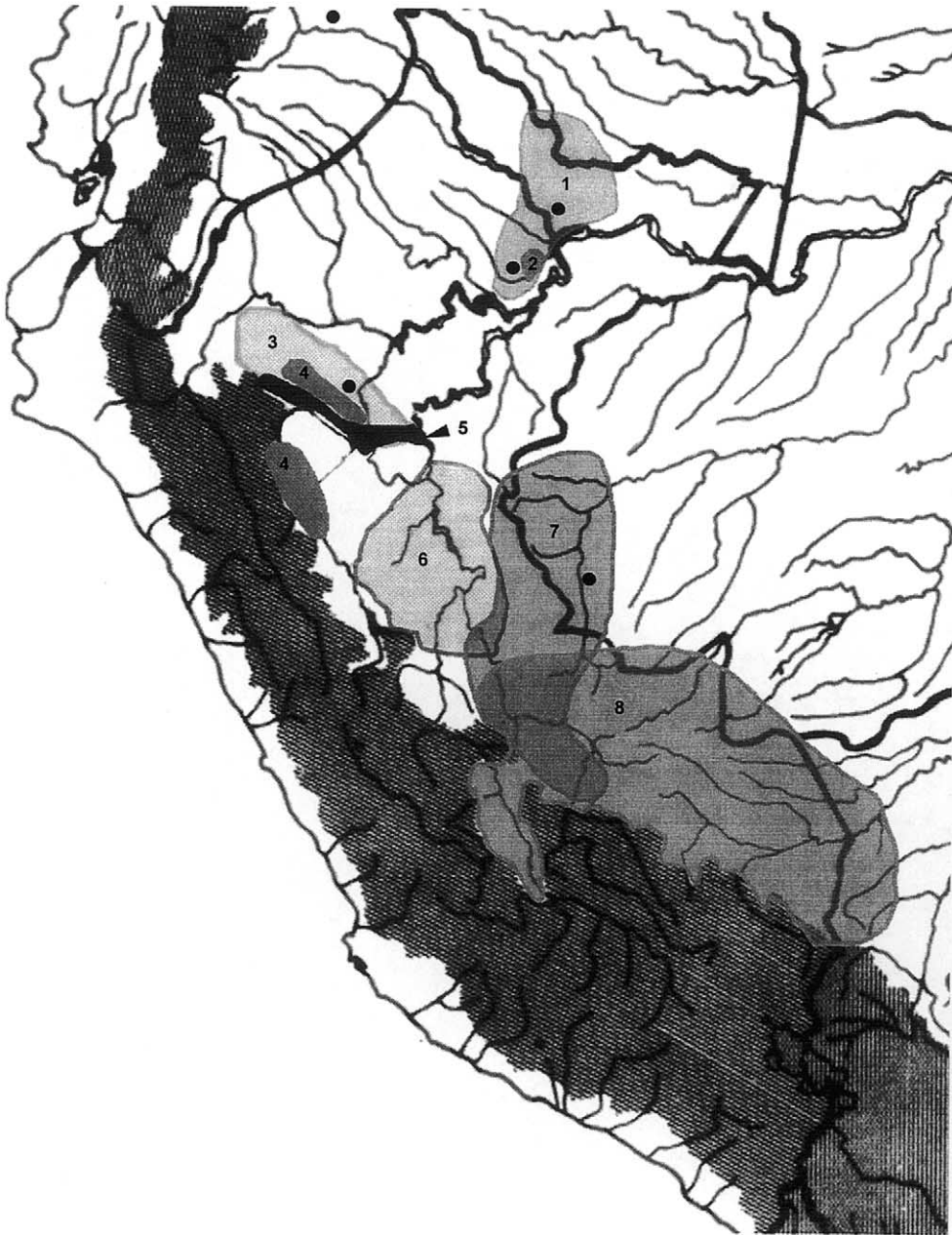


Fig. 1. Distribution of members of the *D. ventrimaculatus* species group in western Amazonia. Species ranges (after Schulte, in preparation) are as follows: (1) *D. reticulatus*; (2) *D. amazonicus*; (3) *D. imitator*; (4) *D. variabilis*; (5) *D. fantasticus*; (6) *D. lamasi*; (7) *D. vanzolinii*; (8) *D. biolat*. Black dots represent approximate collection localities for specimens of *D. ventrimaculatus* used in this study. *Dendrobates ventrimaculatus* is distributed throughout northwestern Amazonia and also occurs in isolated populations in central and eastern Amazonia (distribution not shown).

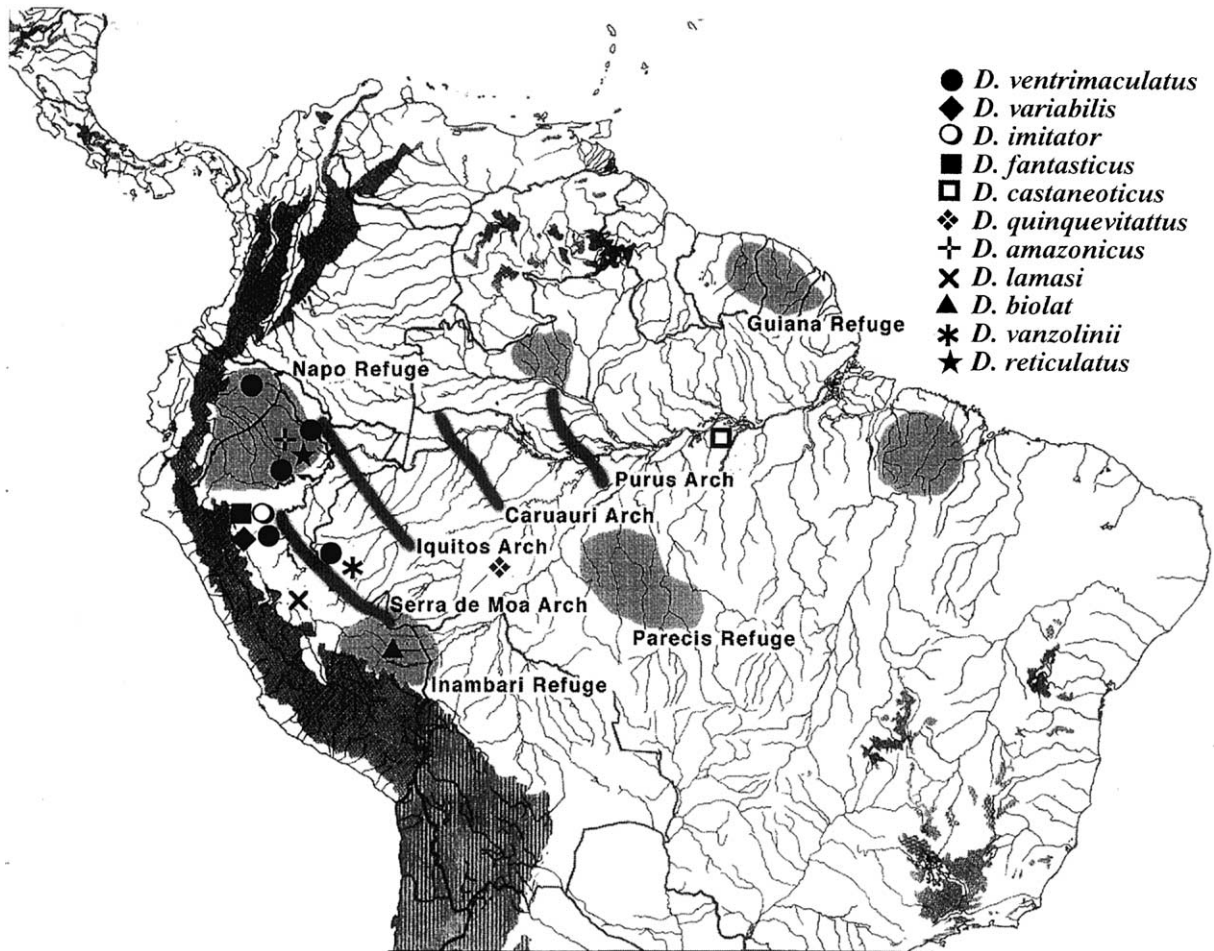


Fig. 2. Sampling locations for the specimens used in the phylogenetic analysis, and geographic barriers proposed by the refuge hypothesis and the Paleogeographic Barrier hypothesis. Refuges are shown as light gray regions and major ancient arches are shown as darkened lines.

The molecular phylogenetic analyses of these frogs in a geographic context can also provide opportunities to test predictions from hypotheses concerning diversification in Amazonia. Amphibians are small and usually exhibit relatively low vagility (Duellman, 1982). Dendrobatid frogs have a forest mode of reproduction and are not only restricted to relatively humid climates, but are limited to specific habitats. Each species of *Dendrobates* is dependent on small pools of water (sometimes associated with specific species of plants) for their tadpoles. Hence they should be directly affected by climatic shifts imposing vegetational changes, as suggested by some of the hypotheses proposed to explain diversity. Because poison frogs of the genus *Dendrobates* range across much of Amazonia, and span a variety of geographic barriers, these frogs also provide an opportunity to examine hypotheses concerning the influence of specific kinds of barriers on genetic diversification.

A variety of hypotheses have been proposed to explain the elevated species diversity in the Amazon Basin (Gascon et al., 2000; Moritz et al., 2000). Many of these

hypotheses propose specific isolating barriers as mechanisms that generated genetic divergence (Patton et al., 1994). Genetic isolation and subsequent speciation usually depend on the formation of extrinsic barriers to gene flow (Mayr, 1942). Employing phylogeographic analysis, it is possible to test the effectiveness of hypothetical barriers to gene flow in Amazonia (Avice, 2000).

Several paleogeographic barriers have been proposed as important barriers to gene flow in Amazonia. The orogeny of the Andes and the resulting arches (now mostly eroded) (Fig. 2), coupled with marine incursions dividing the Amazon basin (Räsänen et al., 1995), have been hypothesized to be important vicariant events causing genetic divergence among species and populations (Patton and da Silva, 1998). An important prediction of this hypothesis is that species or haplotype assemblages should demonstrate monophyly between arches, and arches should reflect points of ancient divergence of species (Patton and da Silva, 1998). Several authors have found evidence to support this hypothesis in rodent and marsupial species (Patton and da Silva,

1998), and frogs (Gascon et al., 1998; Loughheed et al., 1999).

Haffer (1969, 1990) proposed that tropical forests expanded and contracted during glacial cycles (Refuge Hypothesis). These contractions sundered the forest into small islands or isolated refugia, which promoted divergence and speciation. Secondary contact occurred with the expansion of the forests associated with interglacial periods. Repeated isolation led to divergence, speciation, and genetic isolation at secondary contact. Haffer (1997) predicted that levels of divergence would be roughly equivalent between each of the refugia shown in Fig. 2. The Refuge Hypothesis has been investigated by a number of researchers and has been the focus of considerable debate (Brown, 1982; Froehlich et al., 1991; Nores, 1999; Prance, 1982; Prance, 1973; Räsänen et al., 1991; Vanzolini, 1970).

Duellman (1982) proposed a hypothesis similar to Haffer's (1969) Refuge Hypothesis, but specific to anurans. Reproductive modes that depend on terrestrial pools of water typically confine frogs and toads to high humidity environments (Duellman, 1982). Duellman (1982) hypothesized that the most humid regions of rainforest were retained at mountain bases during glaciation and served as amphibian refugia. Duellman's (1982) hypothesis predicts divergence will be higher among species and populations in the highland regions, and that lowland species will be derived from highland ancestry.

Wallace (1853) first proposed that major rivers divided Amazonia into four biogeographic regions. The modern formulation of this "Riverine Barrier" hypothesis (Sick, 1967) proposes that gene flow in Amazonia is restricted by the formation of rivers in regions where forests were previously uninterrupted. This hypothesis predicts that increased river width will result in increased divergence, that populations on each side of a river should form monophyletic groups, and that gene flow should be higher at headwater regions (Capparella, 1988; Gascon et al., 1998). Evidence for and against this hypothesis has been published (e.g., Capparella, 1988; Patton and da Silva, 1998).

Examination of genetic divergence across populations or groups from a variety of taxa is necessary to test these biogeographic hypotheses (Gascon et al., 1998). Models of vicariance predict that divergence between populations or closely related species should reflect the presence of specific biogeographic barriers within a geographic region (Patton and da Silva, 1998). Here we investigate phylogenetic relationships and genetic divergence among populations and closely related species of Amazonian *Dendrobates* to test predictions derived from these different biogeographic hypotheses. Ultimately, this should contribute to a broader understanding of Amazonian biodiversity.

2. Methods

2.1. Sample collection

Tissue samples were collected in the field by one of the authors (with the exception of the samples from Brazil) at the locations listed in Table 1. Samples were generally taken as toe clips from each frog but a few samples were from tail tips of tadpoles. Samples from Brazil were collected by Dr. J.P. Caldwell and were obtained from Louisiana State University Museum of Natural Sciences Collection of Genetic Resources as a tissue grant to the corresponding author. The general distributions of each species analyzed in this study (except *D. quinquevittatus* and *D. castaneoticus*) are shown in Fig. 1, and the sampling locations are shown in Fig. 2. Representative voucher specimens for each species and population utilized in this study are maintained by R. Schulte, at the Instituto de Investigación de la Biología de las Cordilleras Orientales, in Tarapoto, Peru.

2.2. DNA extraction, DNA amplification, sequencing

Genomic DNA was extracted from tissue samples preserved in high concentration salt buffer (DMSO/NaCl/EDTA) with the Qiagen DNeasy Tissue Kit. For the 16S ribosomal RNA (rRNA), 12S rRNA, cytochrome *b*, and cytochrome oxidase I mitochondrial gene regions, DNA samples were amplified using DNA primers and protocols described in Clough and Summers (2000), Summers et al. (1999), Symula et al. (2001). We used the following primer sets: 16s: LGL 381, LGL 286 (Bickham et al., 1996); 12s: 12SA-L, 12SB-H (Kocher et al., 1989), Df12SA, Df12SB (Symula et al., 2001); cytochrome *b*: CB1-L, CB2-H (Palumbi et al., 1991); KSCYB(A)1-L, KSCYB(C)L, KSCYB1-H (Clough and Summers, 2000); cytochrome oxidase I: CO1A, CO1F (Palumbi et al., 1991). DfCO1A, DfCO1B, DiCO1A, DiCO1B (Symula et al., 2001). Cytochrome oxidase I was not sequenced for *D. quinquevittatus* and *Dendrobates vanzolinii*.

PCR amplifications were purified with the Qiagen's QIAquick PCR Purification Kit. Products were sequenced using Applied Biosystems' (ABI) Prizm Sequencing Kit. Samples were then prepared for sequencing as in Clough and Summers (2000).

2.3. Sequence analysis

Each sample was sequenced in both directions and complementary sequences were aligned using Autoassembler version 1.4.0 (ABI 1995). Consensus sequences were transferred to Gene Jockey (Taylor, 1990) for alignment with a sequence from the same region from a different individual. We translated the protein coding

Table 1
Species, collection localities, altitudes, and GPS data for the samples

Species	Location	Altitude	Position
<i>D. amazonicus</i>	Almendras, Loreto, Peru (1)	Lowland	S 3°50'2.8"–W 73°22'32.1"
<i>D. biolat</i>	Tambopata, Madre de Dios, Peru (10)	Lowland	
<i>D. castaneoticus</i>	101 km South, 15 km East of Santarem, Para, Brazil (5)	Lowland	
<i>D. castaneoticus</i>	101 km South, 15 km East of Santarem, Para, Brazil (6)	Lowland	S 3°9'2.4"–W 54°50'32.9"
<i>D. fantasticus</i>	Taropoto, San Martin, Peru (15)	Montane	
<i>D. fantasticus</i>	Sauce, San Martin, Peru (14)	Montane	
<i>D. fantasticus</i>	Huallaga Canyon, San Martin, Peru (16)	Montane	S 6°34'26.4"–W 75°57'54.5"
<i>D. histrionicus</i>	Santo Domingo, Pichincha, Ecuador		
<i>D. imitator</i>	Taropoto, San Martin, Peru (13)	Montane	
<i>D. imitator</i>	Huallaga Canyon, San Martin, Peru (11)	Montane	S 6°34'26.4"–W 75°57'54.5"
<i>D. imitator</i>	Yurimaguas, Loreto, Peru (12)	Lowland	
<i>D. lamasi</i>	From exact paratype locality, Tingo Maria, Huanuco, Peru (9)	Highland	
<i>D. leucomelas</i>	Tabogan, Amazonas, Venezuela		
<i>D. quinquevittatus</i>	Rio Ituxi at the Madeireira Scheffer, left bank, Amazonas, Brazil (4)	Lowland	S 8°20'47.0"–W 65°42'57.9"
<i>D. reticulatus</i>	Nanay River, Loreto, Peru (3)	Lowland	
<i>D. reticulatus</i>	Varrillal, Loreto, Peru (2)	Lowland	S 3°53'28.5"–W 73°20'52.7"
<i>D. vanzolinii</i>	Porto Walter, Acre, Brazil	Lowland	S 8°15'31.2"–W 72°46'37.1"
<i>D. variabilis</i>	Tarapoto, San Martin, Peru (18)	Montane	
<i>D. ventrimaculatus</i>	Porto Walter, Acre, Brazil (21)	Lowland	
<i>D. ventrimaculatus</i>	Yurimaguas, Loreto, Peru (17)	Lowland	S 6°12'44.2"–W 76°13'33.7"
<i>D. ventrimaculatus</i>	Pompeya, Sucumbios, Ecuador (19)	Lowland	
<i>D. ventrimaculatus</i>	Near ACEER camp, north bank of Napo River, Loreto, Peru (20)	Lowland	
<i>D. ventrimaculatus</i>	From across Itaya river going to Nauta, Loreto, Peru	Lowland	S 4°16'27.2"–W 73°30'45.7"
<i>D. ventrimaculatus</i>	Porto Walter, Acre, Brazil (22)	Lowland	
<i>D. ventrimaculatus</i>	Allpahuayo, km 28 on road from Iquitos to Nauta, Loreto, Peru (7)	Lowland	
<i>Dendrobates</i> species	From across Itaya River going to Nauta, Loreto, Peru (8)	Lowland	S 4°16'27.2"–W 73°30'45.7"

Numbers in parentheses refer to sample numbers in Appendix A (a).

sequences to confirm that they were in proper reading frame.

We aligned the DNA sequences with Clustal X (Thompson et al., 1997). For the cytochrome oxidase I and cytochrome *b* gene regions, alignments were unambiguous, with no gaps. For the 16S rRNA and 12S rRNA gene regions, a few regions of ambiguous alignment were removed from the analysis. Unambiguous, informative gaps were coded as transversions in the analysis. A single informative gap was found in the 12S rRNA gene region, and one was found in the 16S rRNA gene region.

To determine whether secondary structure of the rRNA sequences provided additional alignment information, we compared 12S and 16S rRNA sequences to a previously determined secondary structure from piranha sequence (Ortí and Meyer, 1997). One sequence from each dendrobatid species was aligned to piranha sequence. Stems were identified first by aligning sequences from one of each of the sampled taxa to the piranha sequence and then checking to insure the two strands were complementary, allowing for mismatches as discussed by Kjer (1995). We checked the rRNA gene regions to verify that there were no gaps in proposed stem regions, and we used stem regions to check for accurate sequencing (Kjer, 1995).

Sequences for *Dendrobates ventrimaculatus* and *Dendrobates histrionicus* from Ecuador, *D. vanzolinii*

from Brazil, and *Dendrobates leucomelas* from Venezuela were taken from previously compiled data sets (Clough and Summers, 2000) and incorporated into the analysis. GenBank Accession Nos. for the sequences used in this project are as follows: cytochrome oxidase I gene region (mtDNA): AF482815–AF482828; cytochrome *b* gene region (mtDNA): AF482800–AF482814; 16S rRNA gene region (mtDNA): AF482785–AF482799; 12s rRNA gene region (mtDNA): AF482770–AF482784.

2.4. Phylogenetic analysis

We carried out two types of phylogenetic analysis to investigate evolutionary relationships: Maximum Parsimony (MP) and Maximum Likelihood (ML), using the program PAUP* version 4.0 (Swofford, 1999). For the outgroups, we used *D. histrionicus* (Ecuador) and *D. leucomelas* (Venezuela), which fall outside a distinct Amazonian clade within *Dendrobates* (Clough and Summers, 2000).

Phylogenetic analysis was performed on three separate data sets: (1) A data set including all taxa sampled, consisting of DNA sequence data from the 12S rRNA, 16S rRNA, and cytochrome *b* gene regions. (2) A data set including all taxa sampled, with the exception of *D. quinquevittatus* and *D. vanzolinii* and sequence data from all four gene regions (including the cytochrome oxidase I region). (3) A reduced data set for the *D. ventrimaculatus*

populations and closely related species from northwestern Amazonia with southwestern species as outgroups. This data set is restricted to sequences from the cytochrome *b* and cytochrome oxidase I genes. These regions evolve relatively rapidly (Moritz et al., 1987) and hence should be useful in resolving relationships among relatively closely related species and populations.

Parsimony analyses were carried out using stepwise addition with 50 random addition replicates, using tree-bisection and reconnection for branch rearrangement. The analysis employed a dynamic weighting scheme to control for variation in the rates of transition and transversion (Williams and Fitch, 1990). We did not downweight third base pair substitutions in the analysis because saturation plots of Kimura 2-parameter “*p*” distances (Kimura, 1980) revealed substantial signal in both third base pair transversions and transitions (Broughton et al., 2000). Support for particular nodes was investigated with bootstrapping (Felsenstein, 1985), using 2000 replicates.

We performed ML analyses using both combined data sets and data sets for individual gene regions. We used the program Modeltest (Posada and Crandall, 1998) to determine which model of substitution best fit the data, using a preliminary tree derived from ML analysis. Modeltest was also used to derive best fit estimates of base pair frequencies, the proportion of invariant sites and the gamma shape parameter (Posada and Crandall, 1998). The best model was provided by the General Time Reversible model of substitution (Rodríguez et al., 1990), including a gamma shape parameter (Yang, 1996) estimated from the data. Gamma parameters, base composition and a proportion of invariant sites for each of the data sets are presented in Table 2 for the combined data sets. These parameters were used for phylogenetic analysis in PAUP*. For ML analyses, a heuristic search was run with 50 replicates and bootstrapped with 100 replicates for all three data sets and for each of the gene regions separately.

2.5. Hypothesis testing

We tested predictions from four different biogeographic hypotheses: (1) The Paleogeographic Barrier

Hypothesis. (2) The Refuge Hypothesis. (3) The Riverine Barrier Hypothesis. (4) The Montane Refuge Hypothesis.

(1) Under the Paleogeographic Barrier Hypothesis, we expect *D. castaneoticus*, the eastern-most species, to be substantially diverged from the remaining species. *D. castaneoticus* is separated from the western taxa (*D. ventrimaculatus*, *D. imitator*, *D. amazonicus*, *D. reticulatus*, *D. fantasticus*, *D. variabilis*, *D. vanzolinii*, *D. biolat*, *D. lamasi*) by four arches, from west to east: Serra do Moa Arch, Iquitos Arch, Caruauri Arch, and the Purus Arch (Fig. 2). *D. quinquevittatus* is separated from the northwestern populations by the Iquitos and Serra do Moa arches, and from the southwestern populations by the Serra do Moa Arch. *D. quinquevittatus* is also separated from *D. castaneoticus* by the Purus Arch and the Caruauri Arch. We predicted two major clades that show deep phylogenetic divergence and separate eastern taxa versus western taxa. In contrast to the Refuge hypothesis, the Paleogeographic Barrier hypothesis predicts higher levels of divergence between east and west than between north and south.

Four a priori tree topologies (Goldman et al., 2000), three inconsistent, and one consistent with the Paleogeographic Barrier Hypothesis (see below) were constructed with MacClade 3.05 (Maddison and Maddison, 1993). The first two topologies grouped one of the eastern species (*D. castaneoticus* or *D. quinquevittatus*) within a polytomy containing all of the western species, and the third grouped a western species (*D. ventrimaculatus*) with the eastern species. These topologies were compared to the topology grouping *D. castaneoticus* and *D. quinquevittatus* in a clade, with all eastern taxa forming another clade (as a polytomy) using Kishino–Hasegawa (KH) tests (Kishino and Hasegawa, 1989) as implemented in PAUP*. We also compared genetic distances using a student’s *t* test (see below).

(2) The Refuge Hypothesis predicts that species from each different refuge will diverge simultaneously from those in other refugia (Haffer, 1997). Here we present data on species associated with three major refugia: *D. ventrimaculatus*, *D. variabilis*, *D. fantasticus*, *D. amazonicus*, and *D. reticulatus* from the northwest (Napo Refuge region); *D. vanzolinii*, *D. lamasi*, and *D. biolat*

Table 2
ML model parameters for the data sets used to construct phylogenetic trees

Data set	Gamma	Base composition	Prop. invar. sites
Without cytochrome oxidase I	0.5865	A = 0.2914, C = 0.2531 G = 0.1926, T = 0.2629	0.373
All four gene regions	0.5880	A = 0.2849, C = 0.2550 G = 0.1814, T = 0.3541	0.3541
Cytochrome <i>b</i> and cytochrome oxidase I	0.4639	A = 0.3138, C = 0.2225 G = 0.1538, T = 0.3099	0.3173

All parameters were generated using Modeltest (Posada and Crandall, 1998).

from the southwest (Inambari Refuge region); *D. castaneoticus* and *D. quinquevittatus* from central Amazonia (Parecis Refuge region). The Refuge Hypothesis predicts three major groups roughly associated with the three refuges depicted in Fig. 2. Further, these separations of taxa should be accompanied by approximately equal genetic divergence between each refuge (Haffer, 1997). Several species (*D. fantasticus*, *D. variabilis*, and *D. imitator*) occupy ranges between the Napo and the Inambari regions, and were difficult to assign a priori to either the Napo or Inambari refuge region. Hence it was not possible to predict an a priori tree topology for the Refuge Hypothesis. Instead of using topology tests, we compared the differences in average genetic distances (estimated via ML) between taxa occurring in specific geographic regions (east versus west compared to north versus south) with a student's *t* test, using the program Statview.

(3) The Riverine Barrier Hypothesis predicts that populations on the same side of large rivers will be closely related and form monophyletic groups. Our most sensitive test of this hypothesis utilized data from the relatively rapidly evolving cytochrome *b* and cytochrome oxidase I mtDNA regions to investigate divergence among populations of *D. ventrimaculatus* and closely related species in northwestern Amazonia.

(4) Montane Refuge Hypothesis: This hypothesis predicts that divergence will be higher among highland populations and species. It also predicts that lowland species will typically be derived from highland ancestry. We tested these predictions by comparing genetic distances and phylogenetic relationships among highland and lowland species in our dataset, particularly *D. variabilis* and *D. fantasticus* from the highlands and *D. ventrimaculatus*, *D. amazonicus*, *D. reticulatus*, and *D. vanzolinii* from the lowlands (*D. imitator*, *D. lamasi*, and *D. biolat* span highland and lowland habitats).

3. Results and discussion

3.1. Molecular phylogenetics

The final data set for all four gene regions comprised 1598 base pairs (556 from 16S rRNA, 320 from 12S rRNA, 454 from cytochrome oxidase I, and 268 from cytochrome *b*). For the MP analysis of all four gene regions 448 characters were informative. The analysis excluding cytochrome oxidase I had 279 informative characters. ML and MP analyses produced almost identical topologies, but the ML trees had higher bootstrap support for clades with low branch support in MP analyses. Trees shown in Figs. 3–5 are ML topologies with branch length estimates above branches and bootstrap values below branches. These trees also depict the most parsimonious hypotheses.

Fig. 3 shows the ML tree for the analysis without cytochrome oxidase I and with all 25 taxa. Two strongly supported clades were found: one including all of the western taxa and one including three southwestern species *D. lamasi*, *D. biolat*, *D. vanzolinii*, and *D. imitator* from the northwest. The other northwestern species formed a large clade, but there was little resolution within that clade. *D. ventrimaculatus* from Yurimaguas and *D. variabilis* from Tarapoto fall together as sister taxa with 100% bootstrap support and are sister taxa to *D. ventrimaculatus* from Pompeya, Ecuador. All populations of *D. fantasticus* from Tarapoto, Huallaga Canyon and Sauce form a monophyletic group with a bootstrap value of 70%. The Brazilian samples of *D. ventrimaculatus* form a strongly supported clade. Other relationships of taxa within the northern group were ambiguous in this analysis. In the southern group, *D. imitator* forms a monophyletic group with 100% bootstrap support, and *D. vanzolinii* is also strongly supported (100%) as the sister taxon to *D. imitator*. *D. biolat* and *D. lamasi* are sister taxa and form a separate clade with 100% bootstrap support. *D. castaneoticus* and *D. quinquevittatus* form a clade outside of the western clade and outside of the *D. leucomelas* outgroup.

The results of the ML analysis including all four gene regions are shown in Fig. 4. The ML tree is similar to the tree without cytochrome oxidase I, with an eastern taxon (*D. castaneoticus*) and a western clade, but the analysis provides more resolution. *D. castaneoticus* is placed outside *D. leucomelas* with a high bootstrap value. *D. leucomelas* is the apparent sister taxon to the western clade in both MP and ML analyses. Within the western clade there is additional resolution to the tree within the group containing the northern taxa. The northern group is split into two separate clades. The first clade joins *D. reticulatus*, *D. fantasticus*, and *D. ventrimaculatus* from Porto Walter, Brazil. *D. fantasticus* populations fall out together with bootstrap of 95%. Populations of *D. reticulatus* and a specimen of unknown species status (possibly a hybrid between *D. reticulatus* and *D. duellmani*) fall into a single strongly supported clade. Populations of *D. ventrimaculatus* from Porto Walter, Brazil also form a clade with a bootstrap value of 100%. The remaining populations from the northern group fall into a single clade with a bootstrap value of 96%. Within this clade *D. ventrimaculatus* from Yurimaguas and *D. variabilis* from Tarapoto are closely related, and *D. ventrimaculatus* from Pompeya, Ecuador is placed as their sister taxon.

Tables of genetic distances between all taxa for each gene region are provided in Appendix A. One puzzling feature is the high level of genetic divergence between the two specimens of *D. ventrimaculatus* from Porto Walter, Brazil (although these specimens are placed together in our phylogenetic analyses). The explanation for these high levels of divergence awaits further re-

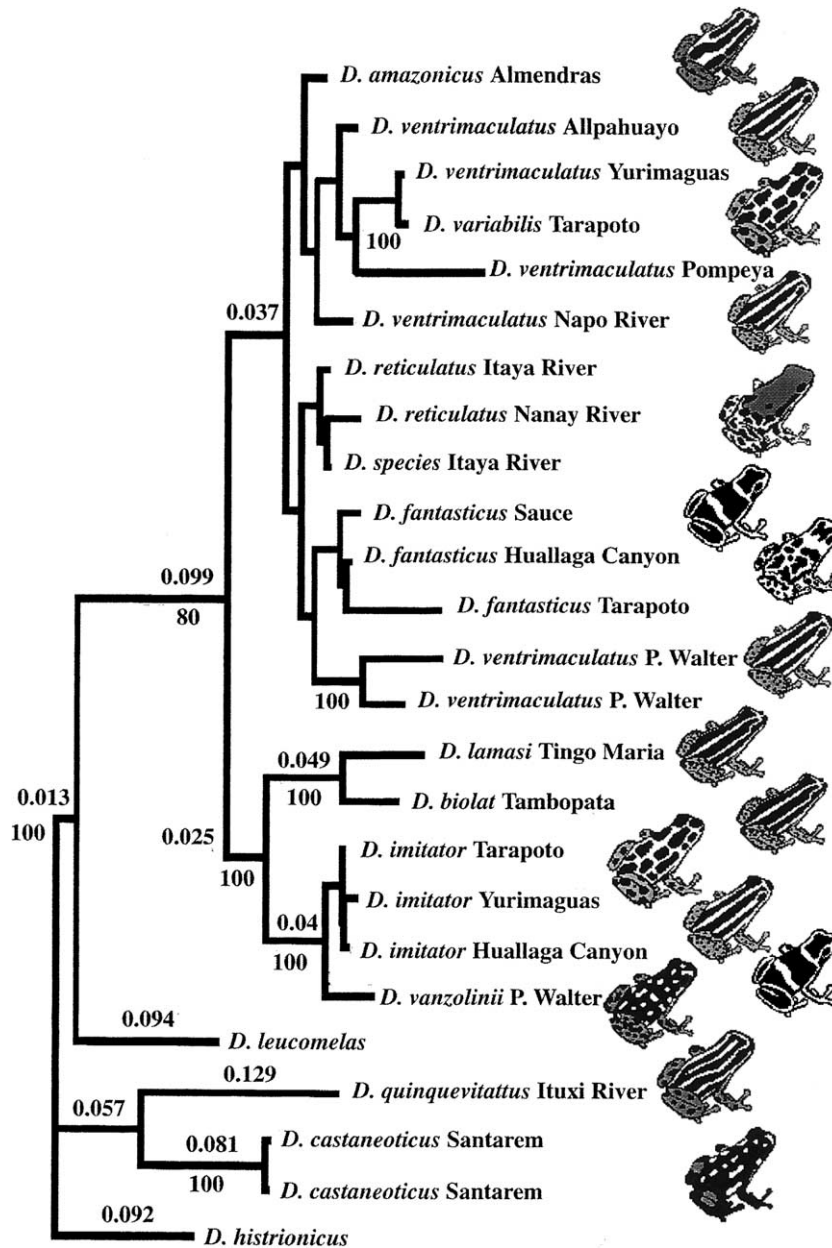


Fig. 3. Phylogram showing the ML tree topology for the analysis of phylogenetic relationships of the *D. ventrimaculatus* group that included 16S rRNA, 12S rRNA, and cytochrome *b* mitochondrial gene regions, but did not include the cytochrome oxidase I gene region. ML branch lengths (fractions) and bootstrap values (whole numbers) are shown adjacent to relevant branches. Only bootstrap values higher than 75% are shown. Silhouettes indicate the color pattern of each of the frogs sampled.

search. ML gene trees are provided in Appendix B. Most of the differences occur in the resolution of the taxa from northwestern Amazonia. Both 16S rRNA and 12S rRNA provide resolution with relatively strong bootstrap support separating the three major clades.

Caldwell and Myers (1990) raised several questions about the organization of the *D. ventrimaculatus* group, particularly concerning the taxonomic status of *D. variabilis*. They argued that it is unclear whether *D. variabilis* warrants specific status. Our analysis indicates

that *D. variabilis* from Tarapoto, Peru and *D. ventrimaculatus* from Yurimaguas, Peru are more closely related to each other than they are to *D. ventrimaculatus* from Pompeya, Ecuador (Figs. 3–5). This is consistent with the hypothesis that *D. variabilis* is a color and pattern variant of *D. ventrimaculatus*. However, there are acoustic differences between the advertisement calls of *D. variabilis* and *D. ventrimaculatus* (Appendix C). Furthermore, *D. variabilis* is restricted to the summits of mid-level mountains, whereas *D. ventrimaculatus* is

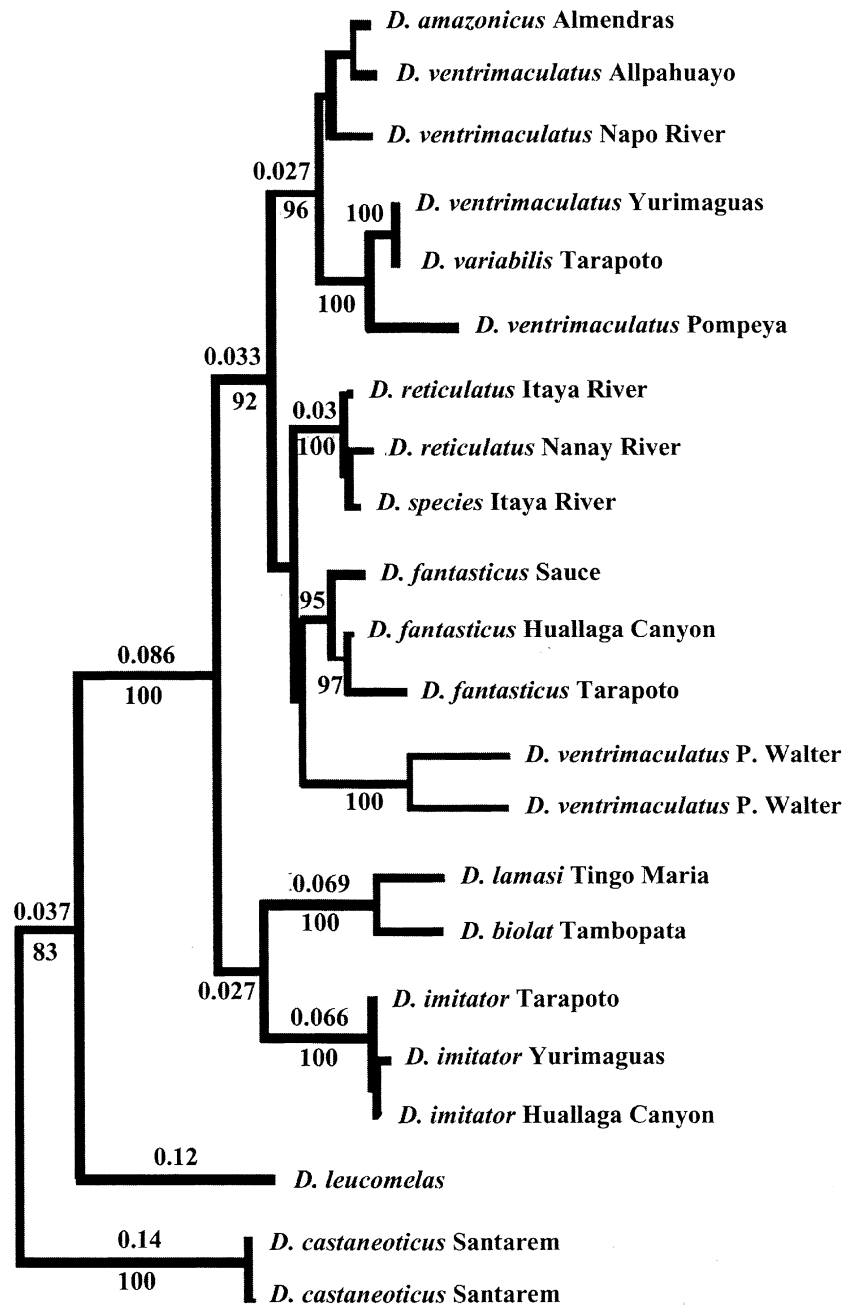


Fig. 4. Phylogram showing the ML tree topology from the analysis of phylogenetic relationships of the *D. ventrimaculatus* group that included 16S rRNA, 12S rRNA, cytochrome *b*, and cytochrome oxidase I gene regions. ML branch lengths and bootstrap values are shown as in Fig. 3.

confined to lowland habitats. We believe that further research (particularly hybridization studies) is warranted before a conclusion on the species status of *D. variabilis* is reached. *D. amazonicus* (Schulte, 1999) also appears closely related to a population of *D. ventrimaculatus* from Allpahuayo, Peru.

Our analysis supports the separation of *D. quinquevittatus* (as defined by Caldwell and Myers, 1990) from the widespread *D. ventrimaculatus* (Figs. 3 and 4). Based on Lynch's (1979) argument that there are

few species distributed widely across major forest regions in Amazonia, populations assigned to *D. ventrimaculatus* may not constitute a single species. Caldwell and Myers (1990) also suggested that *D. ventrimaculatus* may comprise a composite species. Consistent with Caldwell and Myers' (1990) hypothesis, our analysis indicates that populations of *D. ventrimaculatus* do not form a monophyletic group (Fig. 3–5). Rather, *D. ventrimaculatus* from Porto Walter, Brazil appears to be the sister taxon to *D.*

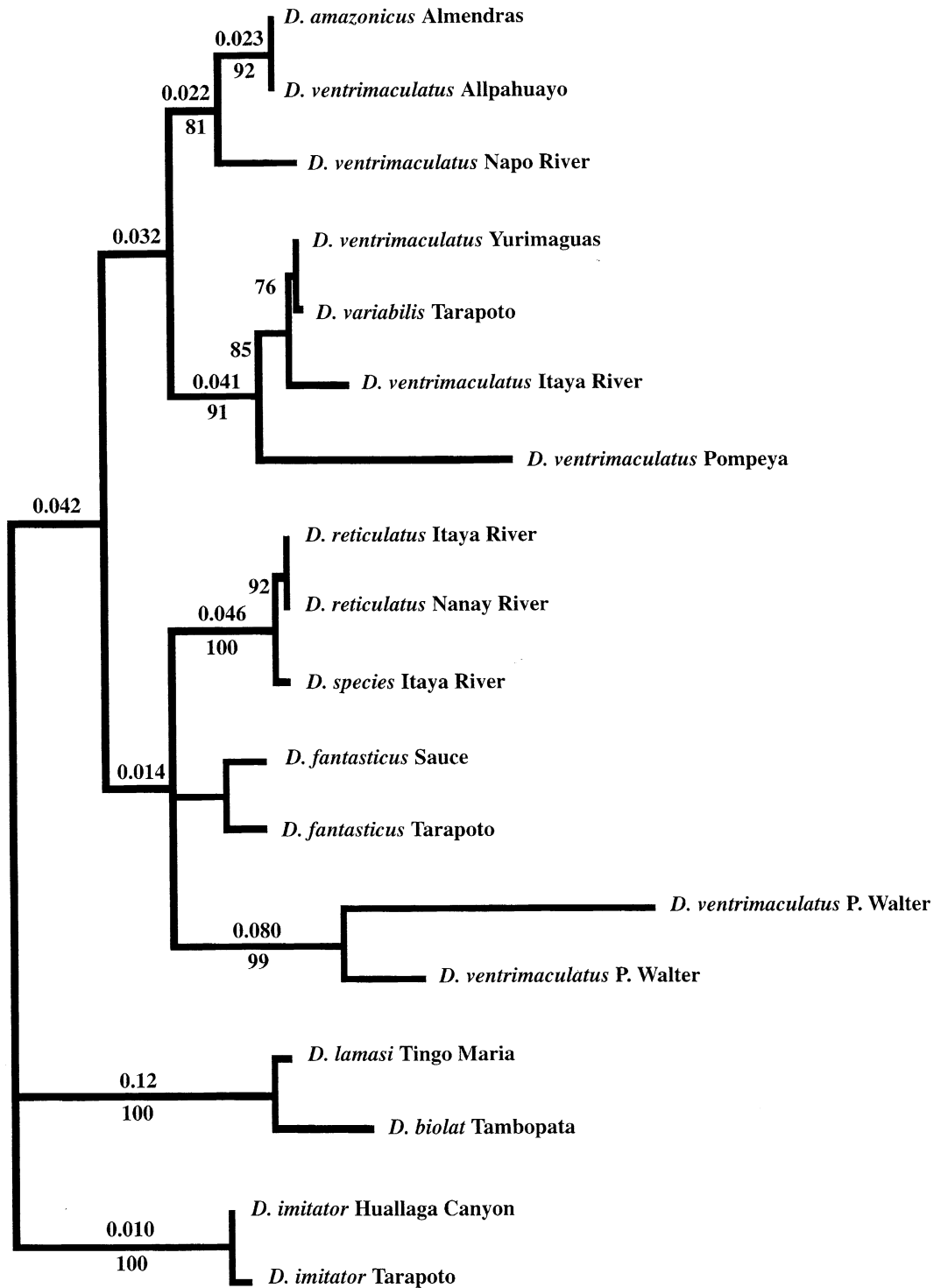


Fig. 5. Phylogram showing the ML tree topology from the analysis of phylogenetic relationships of northwestern populations of the *D. ventrimaculatus* species group. This analysis included only the cytochrome *b* and cytochrome oxidase I mitochondrial gene regions. ML branch lengths and bootstrap values are shown as in Fig. 3.

fantasticus, not to the populations of *D. ventrimaculatus* from Ecuador and Peru.

Populations of *D. ventrimaculatus* from Peru and Ecuador fall into the same clade (Fig. 3–5) although

their status as members of a single species must await clarification of the species status of *D. amazonicus* and *D. variabilis*. *D. ventrimaculatus* appears to be a relatively ancient, widespread color and pattern morph that

has given rise to several different species lineages or variant populations in western Amazonia (*D. fantasticus*, *D. reticulatus*, *D. variabilis*, and *D. amazonicus*).

Although the species range of *D. imitator* is closer to the Napo Refuge, *D. imitator* is more closely related to the southern species *D. vanzolinii*, *D. biolat*, and *D. lamasi* (Figs. 3 and 4). The results of the analyses presented here, combined with previous analyses of population structure in *D. imitator* (Symula et al., 2001) suggest that *D. imitator* populations have recently colonized their current habitats from a southern ancestral stock, and have undergone rapid diversification in color and pattern, matching populations of local species. This provides further support for the hypothesis that *D. imitator* shares color and pattern with its putative models due to mimetic convergence, rather than common ancestry (Symula et al., 2001).

Perhaps the most surprising systematic result from our analyses is that *D. castaneoticus* and *D. quinquevitattus* were placed outside one of the putative out-

groups (*D. leucomelas*). This result should be considered preliminary, and future research should include multiple members from the *D. leucomelas* clade (particularly *Dendrobates auratus*, *Dendrobates tinctorius*, and *Dendrobates azureus*) to see if the result remains the same. It is certainly possible that this entire clade (the members of which live in northern South America and Central America) shares a common ancestor with members of the Western clade than with *D. castaneoticus* and *D. quinquevitattus* but this hypothesis should be tested further before any conclusions are reached.

3.2. Phylogeography

3.2.1. Paleogeographic Barrier Hypothesis

Fig. 6 shows a composite phylogeny from our molecular systematic analyses (incorporating the enhanced resolution provided by the complete data set, but including species for which cytochrome oxidase I data was

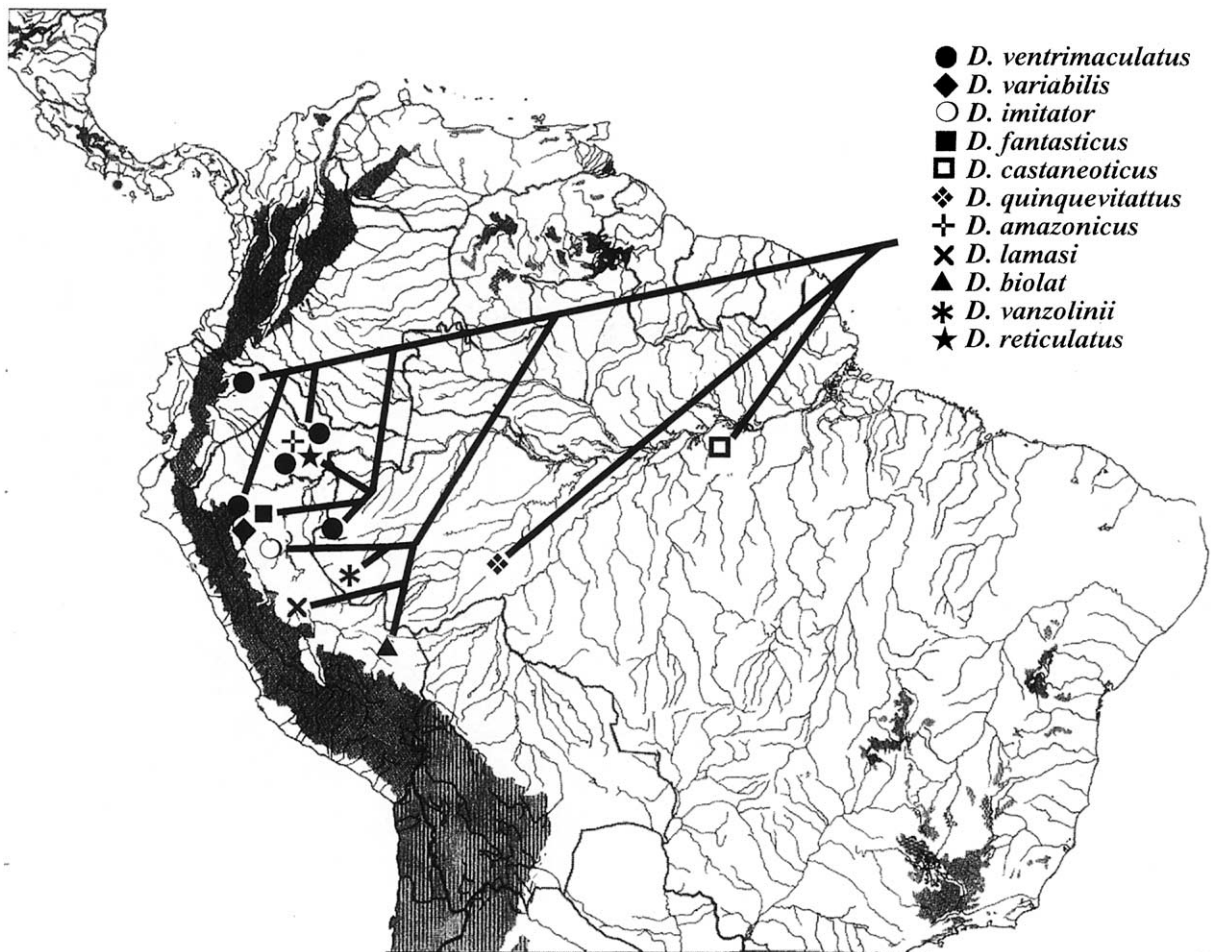


Fig. 6. Depiction of the phylogenetic relationships of the *D. ventrimaculatus* group relative to the geographic location of the populations and species sampled.

not available), overlaid on a map of northern South America to give a phylogeographic perspective. The topology of the tree indicates two major divisions (western versus eastern and northwestern versus southwestern). The deep divergence between eastern and western taxa is consistent with the presence of ancient paleogeographic barriers, as suggested by Räsänen et al. (1990).

The Paleogeographic Barrier Hypothesis predicts higher levels of divergence between eastern and western species than between northern and southern species, due to the presence of ancient barriers to gene flow (Patton and da Silva, 1998). Elevated genetic distances shown in Table 3 support the ancient isolation of these populations. The average ML distance between populations of *D. castaneoticus* and the western populations is $\bar{X} = 0.2951$, $SD = 0.0365$. These populations are separated by the Purus Arch, Carauri Arch the Serra do Moa Arch, and the Iquitos Arch. Populations of *D. quinquevittatus* are separated from the southwestern populations by the Serra do Moa Arch and from the northwestern populations by the Serra do Moa Arch and the Iquitos arch. Genetic distances between these populations are also high ($\bar{X} = 0.3119$, $SD = 0.0272$).

Dendrobates vanzolinii and the westernmost populations of *D. ventrimaculatus* are on the eastern side of the Serra do Moa Arch, but the relatively close genetic relationship between these species and the other members of the western clade (Fig. 3, Appendix A), and the fact that the range of both of these species spans the arch, suggests that they may have crossed the arch recently, or that this arch was not an effective barrier to gene flow. Given that *D. quinquevittatus* does show high divergence with respect to all the western taxa, the former possibility may be more likely.

We compared the average genetic distances between the eastern species (*D. castaneoticus* and *D. quinquevittatus*) and the western species to the average genetic distances between species from the far northwest (*D. amazonicus*, *D. reticulatus*, and *D. ventrimaculatus* from north of the Amazon) and from the far southwest (*D. biolat* and *D. lamasi*). The average genetic distance between the eastern and western species ($\bar{X} = 0.3003$, $SD = 0.0346$) was significantly higher (*t* test, $P < 0.0001$) than the average distance between the northwestern and southwestern species ($\bar{X} = 0.1678$, $SD = 0.0338$). This was not simply a function of geographic distance. For example, the genetic distance between *D. quinquevittatus* and *D. biolat* (0.3119) was substantially higher than that between *D. biolat* and *D. ventrimaculatus* from Pompeya, Ecuador (0.1964), even though the geographic distance between *D. biolat* and *D. quinquevittatus* (621 km) is considerably less than that between *D. biolat* and that population of *D. ventrimaculatus* (985 km).

Time of divergence was calculated using an approximate rate of substitution for cytochrome *b* (0.8–2.5% divergence per million years) (Lougheed et al., 1999) in combination with genetic distances between cytochrome *b* sequences (using the Kimura 2-parameter model to correct for multiple substitution). The range of average divergence times estimated between species from western Amazonia and *D. quinquevittatus* and *D. castaneoticus* was 10–31 million years. These possible times of divergence are very broad, but consistent with the time frame for the formation of both the paleogeographic arches and marine introgressions. The ancient age of divergence among species in our study is consistent with the results of similar analyses in other taxa (Moritz et al., 2000).

Table 3

Average ML distances between some of the species in the analysis, based on 16S rRNA, 12S rRNA, and cytochrome *b* sequence comparisons

Species comparison	Avg. ML dist.	Distance	Proposed barriers
Western to eastern species	0.3003	Approx. 1350 km	Serra do Moa Arch, Iquitos Arch, Carauri Arch, Purus Arch (East vs. West)
Western species to <i>D. castaneoticus</i>	0.2951	Approx. 2100 km	(East vs. West)
Western species to <i>D. quinquevittatus</i>	0.3119	Approx. 600 km	(East vs. West)
Northern species to southern species	0.1678	Approx. 1000 km	Napo and Inambari Refugia (North vs. South)
<i>D. biolat</i> to <i>D. quinquevittatus</i>	0.3119	Approx. 600 km	(East vs. West)
<i>D. biolat</i> to <i>D. ventrimaculatus</i> (Ecuador)	0.1964	Approx. 1200 km	(North vs. South)

Table 4

Kishino–Hasegawa tests

Hypothesis (Tree)	–ln likelihood	Diff –ln likelihood	SD (diff)	<i>t</i>	<i>p</i>
Kishino–Hasegawa tests					
<i>D. castaneoticus</i> (East vs. West)	6761.88052	301.01863	22.77326	13.2181	<0.0001
<i>D. quinquevittatus</i> (East vs. West)	6483.21372	22.35183	18.04052	1.2390	0.2156
<i>D. ventrimaculatus</i> (West vs. East)	6712.95338	252.09149	21.08577	11.9555	<0.0001

The data set without cytochrome oxidase was used to test the a priori phylogenetic hypotheses with alternative tree topologies.

The results of the KH tests comparing topologies are shown in Table 4. Placing *D. castaneoticus* within the western clade results in a significant decrease in likelihood, whereas placing *D. quinquevittatus* in the western clade does not. Placing a member of the western clade (*D. ventrimaculatus*) in a polytomy with *D. castaneoticus* and *D. quinquevittatus* also produces a significant difference in topology. These results are generally consistent with the hypothesis that an ancient barrier has prevented gene flow between eastern and western Amazonia.

Our results are consistent with previous studies on genetic divergence across the Amazon Basin. Patton and da Silva (1998) documented substantive genetic divergence (4–14%) across hypothesized arch locations between populations of rodents and other small mammals that otherwise showed limited (<1%) within population variation. Gascon et al. (1998) found patterns of allozyme divergence in several frog species that were consistent with the hypothesis that the Iquitos Arch has had a significant impact on interpopulation divergence. Finally, a study of mtDNA divergence among populations of the poison frog *Epipedobates femoralis* (currently named *Allobates femoralis*) revealed patterns consistent with the hypothesis that the Iquitos Arch has influenced population genetic differentiation along the Juruá river (Lougheed et al., 1999).

3.2.2. Forest Refuge Hypothesis

Western Amazonian species separate into two distinct northern and southern groups on the basis of genetic affinity, with the exception of *D. imitator* (see above). The separation of the western taxa into southern and northern clades roughly coincides with the the Napo refuge region in the north and the Inambari refuge region in the south, and is consistent with Haffer's (1969) Refuge hypothesis. However, the Refuge hypothesis also predicts that taxa from each of the proposed refuges will be approximately equally diverged from each other (Haffer, 1997). The genetic distances between northern and southern species were significantly lower than those between western and eastern species, as discussed above. These results are not consistent with the prediction of the Refuge hypothesis.

The estimated range of average divergence times between northern and southern species (as defined above) was 8–25 million years, based on cytochrome *b* divergence. Haffer (1997) revised his original hypothesis, under which the refugia were formed by Kroll–Milankovitch cycles in the Pleistocene, to include more ancient cycles of climate change. Our analysis suggests that the divergence between the northern and southern clades took place well before the Pleistocene, but the time of divergence could be consistent with the presence of earlier (Pliocene or Miocene) refugia.

3.2.3. Riverine Barrier Hypothesis

The analysis of populations of *D. ventrimaculatus* and closely related species using the rapidly evolving gene regions produced results that were inconsistent with the Riverine Barrier Hypothesis. The Amazon River should be the largest riverine barrier in the Amazon Basin, but the populations from the same side of major riverine barriers do not form monophyletic groups.

Fig. 5 shows the ML tree of the cytochrome *b* and cytochrome oxidase I regions for the analysis including *D. ventrimaculatus* from the Itaya River, Peru north of the Amazon River. *D. ventrimaculatus* from the Itaya River, Peru is the apparent sister taxon to the populations of *D. ventrimaculatus* from Yurimaguas, Peru and *D. variabilis* from Tarapoto, Peru (which are southwest of the Amazon) with a bootstrap value of 85%. Additionally, these three populations fall into a clade with *D. ventrimaculatus* from Pompeya, Ecuador with a bootstrap of 91%. *D. amazonicus* from Almenbras, Peru is the sister taxon to *D. ventrimaculatus* from Allpahuayo, Peru. These two populations from southwest of the Napo River form a clade with a population of *D. ventrimaculatus* from northeast of the Napo River.

Most recent studies of genetic divergence across rivers in Amazonia have not supported the Riverine Barrier Hypothesis. Patton and his colleagues (e.g. Patton and da Silva, 1998) investigated DNA sequence divergence among populations in seventeen species and species complexes of terra firme rodents. Their results contradicted predictions derived from the Riverine Barrier Hypothesis. Gascon et al. (1998) provided evidence that rivers do not constitute effective barriers to gene flow in the Brazilian lowlands for several different frog species. Lougheed et al. (1999) tested the Riverine Barrier Hypothesis for divergence among populations of the poison frog *A. femoralis*. They found that populations on opposite sides of the Juruá River are not monophyletic, nor is divergence highest at the junction of the Juruá and Amazon Rivers, in contrast to the predictions of the Riverine Barrier Hypothesis.

One reason that rivers may not serve as effective barriers is that river courses are shifting constantly and sometimes undergo major shifts (Lundberg et al., 1998). Geological evidence for the dynamic nature of Amazonian rivers has been presented by Räsänen et al. (1987, 1992). This evidence suggests that populations on one side of a river (even a river with wide flood plains) may be shifted to the other side of the river by changes in the course of the river due to tectonic activity. The only clear effect of a riverine barrier from our research is the strong divergence between populations of *D. fantasticus* on either side of the Huallaga River in Peru (Symula et al., 2001). However, the movement of the Huallaga River is restricted by a

canyon at that point and its course is not as free to change as are lowland rivers.

3.3. Montane Refuge Hypothesis

According to Duellman's (1982) hypothesis montane valleys act as refugia, driving speciation. This hypothesis predicts high levels of divergence between these valleys. Furthermore, Duellman's (1982) hypothesis predicts that lowland species will be derived from highland ancestry. In contrast to this prediction, levels of genetic divergence among highland species were similar in magnitude to those among lowland species (Appendix A) and highland species appear to be derived from lowland ancestry (Figs. 3–5).

There have been few other attempts to test the Montane Refuge hypothesis in frogs. A molecular systematic study of hylid frogs (Chek et al., 2001) revealed deep divergences within lowland populations, contradicting a prediction of this hypothesis.

3.4. Species diversity in northwestern Amazonia

There are two questions that concern the influence of geographic barriers on genetic divergence. First, did the geographic features serve as strong barriers to gene flow? If so, there should be high levels of genetic divergence between species on either side of the geographic barriers. Second, was divergence across the geographic barrier responsible for a major portion of the diversity seen in a clade? Geographic barriers can generate high levels of diversity through several different mechanisms. One of these proposed mechanisms involves repeated vicariance (Avice, 2000). For example, repeated marine introgression and subsidence can disconnect and reconnect areas repeatedly. If this is accompanied by range expansion of newly formed species after each vicariant event, it can result in the repeated formation of new species. This kind of repeated speciation predicts a specific branching pattern in the resulting phylogenetic tree. Pairs of sister taxa should repeatedly span the geographic barrier, and clades should be related across the barrier in a hierarchical manner. Our DNA sequence comparisons provide evidence consistent with an ancient effective barrier to gene flow separating eastern and western Amazonia, and a more recent barrier separating southwestern and northwestern Amazonia. However, the results of our analyses are not consistent with a major role for these ancient barriers in generating the species diversity currently observed in western Amazonia.

There are considerably more species of *Dendrobates* in western Amazonia than in central and eastern Amazonia (Fig. 2). The disparity is even more striking than that shown in the figure, because there are several

more species endemic to western Amazonia that were not included in this study (e.g. *D. duellmani*, *D. flavovittatus*, *D. rubrocephalus*, and *D. sirensis* among others). Species diversity is particularly high in northwestern Amazonia (Fig. 2). Because the degree of divergence among the sampled species in northwestern Amazonia is relatively low compared to divergence between regions (Appendix A), speciation in this region may have been relatively recent. The evidence presented here for an association between genetic divergence and the presence of geographic barriers does not provide an explanation for multiple speciation events or for high levels of species diversity in northwestern Amazonia.

The high levels of overall species diversity of northwestern Amazonia may be influenced by ecological heterogeneity. Certainly, the divergence of highland species from lowland ancestry (as suggested by our results) is consistent with the possibility of speciation driven by ecological gradients or discontinuities. Evidence for this kind of effect has been found previously, both in Amazonia and elsewhere (reviewed by Moritz et al., 2000).

Ecological differences may also influence species diversity in the Amazonian lowlands. Traditionally, the Amazon basin has been viewed as species rich, but with relatively little differentiation among habitats and with low regional diversity (Tuomisto et al., 1995). Recently, scientists have argued that this impression is misleading and may be due to a lack of careful analysis of regional diversity (Tuomisto et al., 1995). A variety of techniques are currently being used to quantify landscape heterogeneity in northwestern Amazonia, including satellite image analysis, geological surveys, and field studies of regional plant biodiversity (e.g., Ruokolainen et al., 1997; Tuomisto et al., 1995). These studies have revealed that levels of regional habitat diversity are much higher than previously believed, which could lead to high rates of ecological speciation (Schluter, 1998). Testing this hypothesis will require careful evaluation of the association between habitat differentiation and poison frog species diversity in Amazonia.

Acknowledgments

We thank John Stiller, Trip Lamb, and John Wiley, and three anonymous reviewers for comments on previous versions of the manuscript. We thank Dr. J.P. Caldwell and the Louisiana State University Museum of Natural Sciences Collection of Genetic Resources for tissue samples. Tissues obtained by Dr. Caldwell were collected during expeditions funded by NSF grants DEB-9200779 and DEB-9505518 to L.J. Vitt and J.P. Caldwell.

Appendix A

Genetic distance matrices for each gene region: (a) 16S rRNA, (b) 12S rRNA, (c) cytochrome *b*, (d) cytochrome oxidase I

(a) Uncorrected p distances calculated on the basis of 16S rRNA mtDNA sequence divergence

	1	2	3	4	5	6	7	8
1	–							
2	0.01426	–						
3	0.05116	0.04311	–					
4	0.15839	0.15609	0.16342	–				
5	0.14219	0.14134	0.14823	0.09519	–			
6	0.14246	0.14143	0.14845	0.09388	0	–		
7	0.06434	0.05892	0.04877	0.16682	0.15223	0.15306	–	
8	0.01182	0.0021	0.04023	0.15123	0.13674	0.13727	0.05591	–
9	0.10502	0.10096	0.10106	0.17416	0.17405	0.17479	0.11005	0.09747
10	0.05775	0.05037	0.06161	0.15556	0.14761	0.14835	0.06473	0.04743
11	0.07875	0.07299	0.08343	0.14907	0.14044	0.14066	0.09647	0.0694
12	0.09167	0.08224	0.08659	0.16058	0.14795	0.15059	0.09581	0.08096
13	0.08225	0.0759	0.08205	0.14983	0.13954	0.14209	0.09358	0.07252
14	0.03691	0.03395	0.05542	0.15921	0.15294	0.15568	0.06687	0.0313
15	0.03222	0.0253	0.04881	0.15613	0.14571	0.14628	0.06032	0.02282
16	0.04398	0.03116	0.05844	0.16428	0.16177	0.15975	0.07045	0.03275
17	0.05979	0.05502	0.05086	0.16289	0.14839	0.14903	0.01465	0.05195
18	0.06152	0.0578	0.04954	0.17036	0.15569	0.15649	0.01555	0.05469
19	0.04813	0.04411	0.04216	0.15331	0.13904	0.13961	0.01864	0.04124
20	0.03218	0.02941	0.02322	0.1554	0.14091	0.14152	0.03936	0.0268
21	0.06673	0.05924	0.07267	0.17441	0.16376	0.16653	0.08159	0.05632
22	0.07204	0.06392	0.07974	0.19084	0.18198	0.18491	0.09053	0.06313
	9	10	11	12	13	14	15	16
9 TINGO1A	–							
10 TAMBO1A	0.0702	–						
11 HCQ13C1	0.07709	0.06975	–					
12 NYUR1H5	0.08869	0.0776	0.01339	–				
13 TYSS7G2	0.08223	0.07078	0.00888	0.01872	–			
14 NSAU1D1	0.09397	0.04338	0.07454	0.08777	0.08556	–		
15 TY267E1	0.09364	0.03672	0.06976	0.08119	0.07686	0.01246	–	
16 MTSL3F1	0.10294	0.0442	0.07805	0.09187	0.08698	0.01665	0.01176	–
17 NBON1B1	0.10846	0.06486	0.09224	0.10027	0.0917	0.0628	0.05414	0.06335
18 TY132A1	0.10965	0.06456	0.09382	0.09324	0.09302	0.06869	0.05968	0.07038
19 POMP1A	0.1056	0.05795	0.07811	0.09123	0.08078	0.05415	0.04555	0.05605
20 NAPO4A	0.0888	0.04943	0.07357	0.08709	0.07666	0.04374	0.0352	0.04188
21 H13755	0.1152	0.078	0.09294	0.09662	0.09229	0.06097	0.05227	0.06404
22 H13770	0.11822	0.08505	0.10059	0.09956	0.10146	0.07208	0.06331	0.07899
	17	18	19	20	21	22		
17 NBON1B1	–							
18 TY132A1	0.01593	–						
19 POMP1A	0.01454	0.01562	–					
20 NAPO4A	0.03531	0.0375	0.0268	–				
21 H13755	0.07998	0.08054	0.07306	0.0584	–			
22 H13770	0.08883	0.07596	0.07994	0.06729	0.02739	–		

Appendix A (continued)

(b) Uncorrected p distances calculated on the basis of 12SrRNA mtDNA sequence divergence

	1	2	3	4	5	6	7	8
1 DAMA5A	–							
2 ITY1B	0.02121	–						
3 NANA3A	0.02121	0	–					
4 H15389	0.09355	0.1039	0.1039	–				
5 H15185	0.09588	0.10141	0.10141	0.12807	–			
6 H15243	0.0998	0.10424	0.10424	0.13073	0.00329	–		
7 ALLPA10A	0	0.02273	0.02273	0.0944	0.09831	0.10122	–	
8 ITY6AP2	0.02121	0	0	0.1039	0.10141	0.10424	0.02273	–
9 TINGO1A	0.07218	0.08472	0.08472	0.09756	0.13765	0.14036	0.07508	0.08472
10 TAMBO1A	0.06116	0.07536	0.07536	0.09136	0.1218	0.12465	0.06563	0.07536
11 HCQ13C1	0.0532	0.06818	0.06818	0.09091	0.11443	0.11728	0.05854	0.06818
12 NYUR1H5	0.05319	0.07497	0.07497	0.09758	0.12136	0.12416	0.06533	0.07497
13 TYSS7G2	0.0532	0.06818	0.06818	0.09091	0.11443	0.11728	0.05854	0.06818
14 NSAU1D1	0.01067	0.01967	0.01967	0.09815	0.09895	0.10183	0.0164	0.01967
15 TY267E1	0.00724	0.01679	0.01679	0.0965	0.09001	0.08979	0.01316	0.01679
16 MTSL3F1	0.00713	0.01961	0.01961	0.09839	0.09215	0.09207	0.01644	0.01961
17 NBON1B1	0.01846	0.03259	0.03259	0.09794	0.10532	0.10816	0.01634	0.03259
18 TY132A1	0.01846	0.03259	0.03259	0.09794	0.10532	0.10816	0.01634	0.03259
19 POMP1A	0.01467	0.02281	0.02281	0.08815	0.09545	0.09831	0.01306	0.02281
20 NAPO4A	0.01438	0.02954	0.02954	0.09161	0.09566	0.09848	0.01316	0.02954
21 H13755	0.0288	0.03267	0.03267	0.09818	0.09248	0.09523	0.02624	0.03267
22 H13770	0.01774	0.02603	0.02603	0.09787	0.09869	0.10158	0.02287	0.02603
	9	10	11	12	13	14	15	16
9 TINGO1A	–							
10 TAMBO1A	0.04924	–						
11 HCQ13C1	0.04556	0.00649	–					
12 NYUR1H5	0.05227	0.01299	0.00649	–				
13 TYSS7G2	0.04556	0.00649	0	0.00649	–			
14 NSAU1D1	0.0754	0.06604	0.05884	0.06565	0.05884	–		
15 TY267E1	0.08022	0.07048	0.06295	0.06997	0.06295	0.00664	–	
16 MTSL3F1	0.08197	0.07268	0.06557	0.07238	0.06557	0.0098	0	–
17 NBON1B1	0.08168	0.07234	0.06523	0.07203	0.06523	0.03273	0.02998	0.03267
18 TY132A1	0.08168	0.07234	0.06523	0.07203	0.06523	0.03273	0.02998	0.03267
19 POMP1A	0.07189	0.06247	0.05545	0.0622	0.05545	0.02295	0.02009	0.02285
20 NAPO4A	0.08199	0.06593	0.05889	0.06566	0.05889	0.02288	0.0198	0.01973
21 H13755	0.07858	0.06916	0.06213	0.06889	0.06213	0.03603	0.03316	0.03617
22 H13770	0.07182	0.07233	0.06517	0.07194	0.06517	0.01968	0.02338	0.02617
	17	18	19	20	21			
17 NBON1B1	–							
18 TY132A1	0	–						
19 POMP1A	0.00977	0.00977	–					
20 NAPO4A	0.02947	0.02947	0.0197	–				
21 H13755	0.03264	0.03264	0.02283	0.03274	–			
22 H13770	0.03916	0.03916	0.02937	0.02953	0.02939			

Appendix A (continued)

(c) Uncorrected p distances calculated on the basis of cytochrome b mtDNA sequence divergence

	1	2	3	4	5	6	7	8
1 DAMA5A	–							
2 ITY1B	0.11567	–						
3 NANA3A	0.11661	0	–					
4 H15389	0.18192	0.20447	0.20638	–				
5 H15185	0.18284	0.22015	0.2179	0.17077	–			
6 H15243	0.1506	0.19625	0.19722	0.17602	0.01953	–		
7 ALLPA10A	0	0.11567	0.11661	0.18192	0.18284	0.1506	–	
8 ITY6AP2	0.11567	0.01493	0.01506	0.19689	0.22015	0.19637	0.11567	–
9 TINGO1A	0.17164	0.15299	0.15433	0.23501	0.23507	0.20384	0.17164	0.16418
10 TAMBO1A	0.1791	0.17537	0.17681	0.23126	0.23881	0.20778	0.1791	0.18657
11 HCQ13C1	0.15672	0.14179	0.13898	0.22317	0.24254	0.22761	0.15672	0.14179
12 NYUR1H5	0.14623	0.13101	0.12806	0.22427	0.23987	0.22453	0.14623	0.13104
13 TYSS7G2	0.1426	0.135	0.13211	0.23194	0.23225	0.2167	0.1426	0.13501
14 NSAU1D1	0.12371	0.08623	0.08306	0.20969	0.20963	0.18672	0.12371	0.08623
15 TY267E1	0.12749	0.08983	0.08654	0.19038	0.20975	0.19007	0.12749	0.08986
16 MTSL3F1	0.19801	0.18694	0.18864	0.19329	0.1934	0.16784	0.19801	0.18699
17 NBON1B1	0.13433	0.15672	0.1578	0.21253	0.22761	0.19709	0.13433	0.16045
18 TY132A1	0.13878	0.16126	0.16237	0.2134	0.23225	0.20184	0.13878	0.165
19 POMP1A	0.25578	0.23283	0.23483	0.25238	0.28221	0.26376	0.25578	0.23289
20 NAPO4A	0.07533	0.10895	0.10983	0.19891	0.19166	0.16306	0.07533	0.11657
21 H13755	0.1306	0.15299	0.15415	0.19711	0.20896	0.19247	0.1306	0.15299
22 H13770	0.11613	0.086	0.08254	0.20837	0.18731	0.16603	0.11613	0.08259
	9	10	11	12	13	14	15	16
9 TINGO1A	–							
10 TAMBO1A	0.04478	–						
11 HCQ13C1	0.16418	0.19403	–					
12 NYUR1H5	0.16113	0.19868	0.01124	–				
13 TYSS7G2	0.16486	0.19491	0.01119	0.00755	–			
14 NSAU1D1	0.16855	0.18346	0.1385	0.13521	0.13919	–		
15 TY267E1	0.18356	0.19864	0.12353	0.12786	0.13164	0.03768	–	
16 MTSL3F1	0.20114	0.21259	0.20518	0.21386	0.20982	0.19512	0.18359	–
17 NBON1B1	0.16791	0.16791	0.18284	0.18739	0.19136	0.11991	0.13862	0.2205
18 TY132A1	0.17233	0.16867	0.18744	0.19204	0.19602	0.12429	0.14306	0.22133
19 POMP1A	0.24088	0.27151	0.23283	0.22981	0.23033	0.24146	0.24893	0.23018
20 NAPO4A	0.17683	0.1844	0.17671	0.17371	0.16248	0.12114	0.13269	0.18801
21 H13755	0.19776	0.19403	0.1903	0.18735	0.17625	0.17232	0.17247	0.2125
22 H13770	0.17597	0.19106	0.16471	0.16168	0.15789	0.08284	0.07521	0.17148
	17	18	19	20	21			
17 NBON1B1	–							
18 TY132A1	0.00378	–						
19 POMP1A	0.27882	0.28399	–					
20 NAPO4A	0.1092	0.11351	0.25003	–				
21 H13755	0.16045	0.16115	0.28262	0.13922	–			
22 H13770	0.16883	0.17334	0.25707	0.11724	0.16853	–		

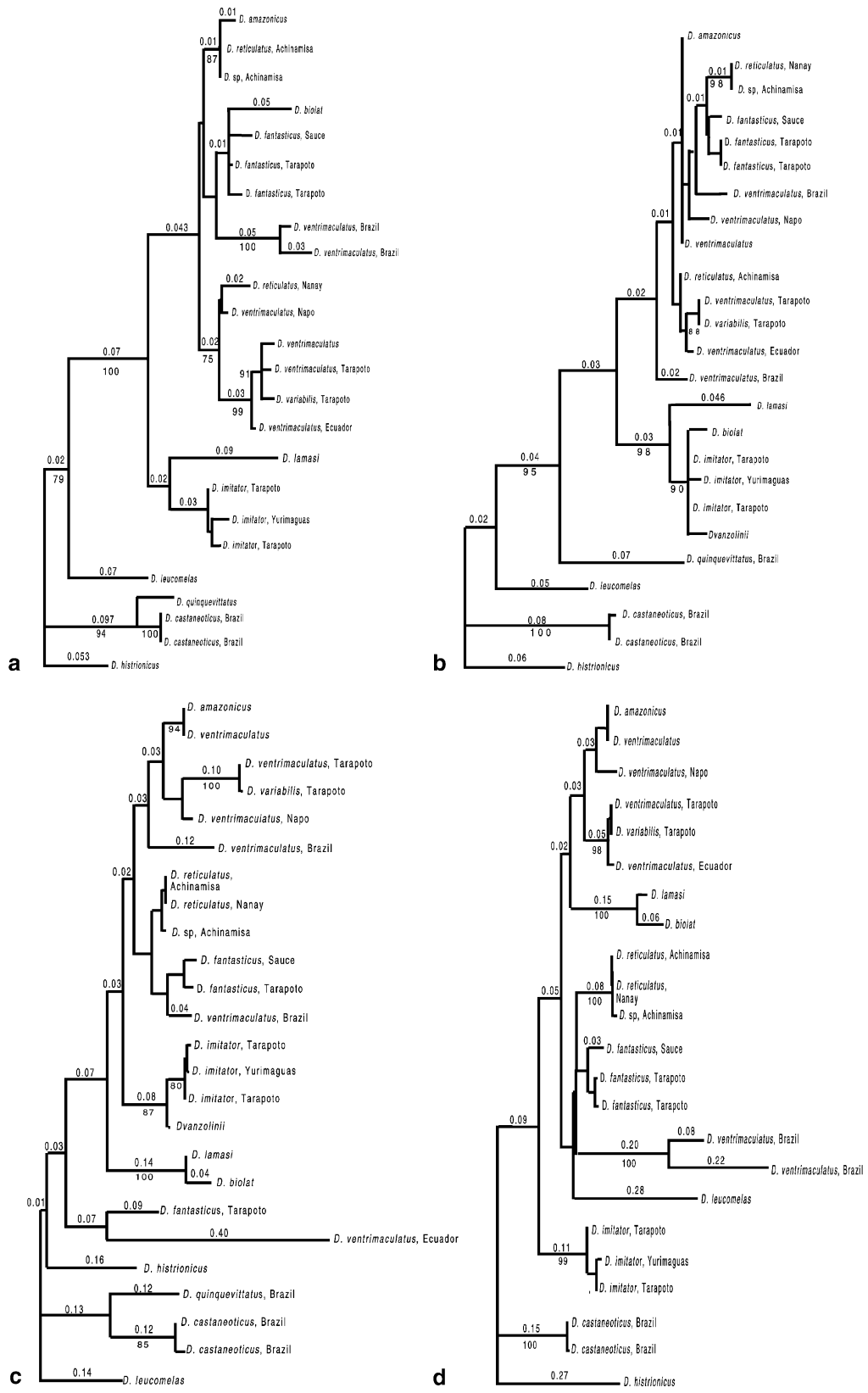
Appendix A (continued)

(d) Uncorrected p distances calculated on the basis of cytochrome oxidase I mtDNA sequence divergence

	1	2	3	4	5	6	7	8
1 DAMA5A	–							
2 ITY1B	0.11917	–						
3 NANA3A	0.11763	0	–					
4 H15185	0.17337	0.18805	0.18529	–				
5 H15243	0.1765	0.19354	0.19128	0.00456	–			
6 ALLPA10A	0.00672	0.12169	0.11884	0.17785	0.17831	–		
7 ITY6AP2	0.12586	0.00905	0.00895	0.18622	0.19676	0.12715	–	
8 TINGO1A	0.12763	0.15752	0.16033	0.19505	0.19907	0.12205	0.16785	–
9 TAMBO1A	0.13955	0.17067	0.17018	0.21036	0.21558	0.13756	0.17861	0.0569
10 HCQ13C1	0.13919	0.14184	0.14672	0.16705	0.17051	0.14066	0.14844	0.15065
11 NYUR1H5	0.14912	0.15368	0.15677	0.17974	0.18278	0.15008	0.16019	0.16557
12 TYSS7G2	0.13942	0.14199	0.14685	0.16726	0.17293	0.1409	0.14858	0.15339
13 NSAU1D1	0.12906	0.08888	0.08945	0.17001	0.1851	0.12829	0.09362	0.14895
14 TY267E1	0.128	0.09235	0.08899	0.16215	0.17906	0.12914	0.09521	0.13913
15 MTSL3F1	0.12996	0.08556	0.08193	0.15966	0.17656	0.13134	0.08829	0.13876
16 NBON1B1	0.0793	0.13062	0.12651	0.17548	0.18314	0.08466	0.13023	0.16398
17 TY132A1	0.07505	0.13322	0.12909	0.17828	0.18583	0.08037	0.13278	0.16215
18 POMP1A	0.0815	0.13271	0.13107	0.18199	0.1853	0.08684	0.13244	0.16607
19 NAPO4A	0.05516	0.13034	0.1309	0.17388	0.17903	0.05795	0.13261	0.14168
20 H13755	0.19633	0.18853	0.18666	0.23827	0.23965	0.19867	0.19211	0.1969
21 H13770	0.22216	0.19565	0.19499	0.23805	0.25616	0.22216	0.19761	0.22367
	9	10	11	12	13	14	15	16
9 TAMBO1A	–							
10 HCQ13C1	0.16727	–						
11 NYUR1H5	0.18009	0.01116	–					
12 TYSS7G2	0.17231	0.00442	0.0111	–				
13 NSAU1D1	0.16249	0.13632	0.14591	0.1367	–			
14 TY267E1	0.15601	0.14626	0.1604	0.14858	0.04014	–		
15 MTSL3F1	0.15366	0.15027	0.1644	0.15257	0.04445	0.00661	–	
16 NBON1B1	0.15802	0.15033	0.16	0.15261	0.13124	0.11703	0.11454	–
17 TY132A1	0.15622	0.15069	0.16039	0.15297	0.12941	0.1151	0.11261	0.0022
18 POMP1A	0.16007	0.15252	0.16214	0.15483	0.14233	0.12368	0.12555	0.01542
19 NAPO4A	0.14678	0.14828	0.1582	0.14846	0.12711	0.11702	0.11688	0.09485
20 H13755	0.20517	0.1946	0.20414	0.19963	0.18487	0.17832	0.17157	0.19393
21 H13770	0.24532	0.26093	0.27597	0.26092	0.18369	0.18708	0.18443	0.23314
	17	18	19	20				
17 TY132A1	–							
18 POMP1A	0.01766	–						
19 NAPO4A	0.09063	0.10144	–					
20 H13755	0.18988	0.19834	0.19871	–				
21 H13770	0.23371	0.23532	0.23813	0.15762				

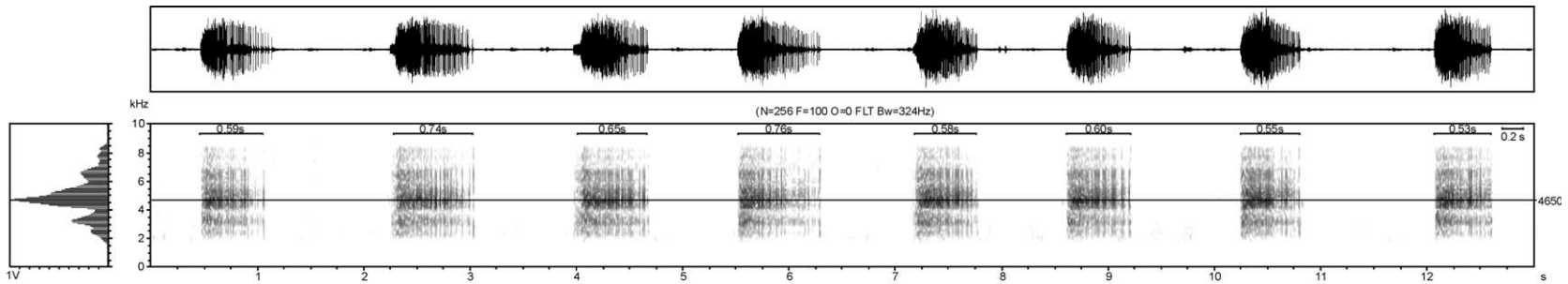
Appendix B

Phylograms showing the tree topologies produced by ML analysis of phylogenetic relationships for each of the gene regions: (a) 16s rRNA, (b) 12s rRNA, (c) cytochrome *b*, (d) cytochrome oxidase I. Values below the branches are bootstrap values and were only shown above 75%. Values above the branches are distances calculated via ML analysis



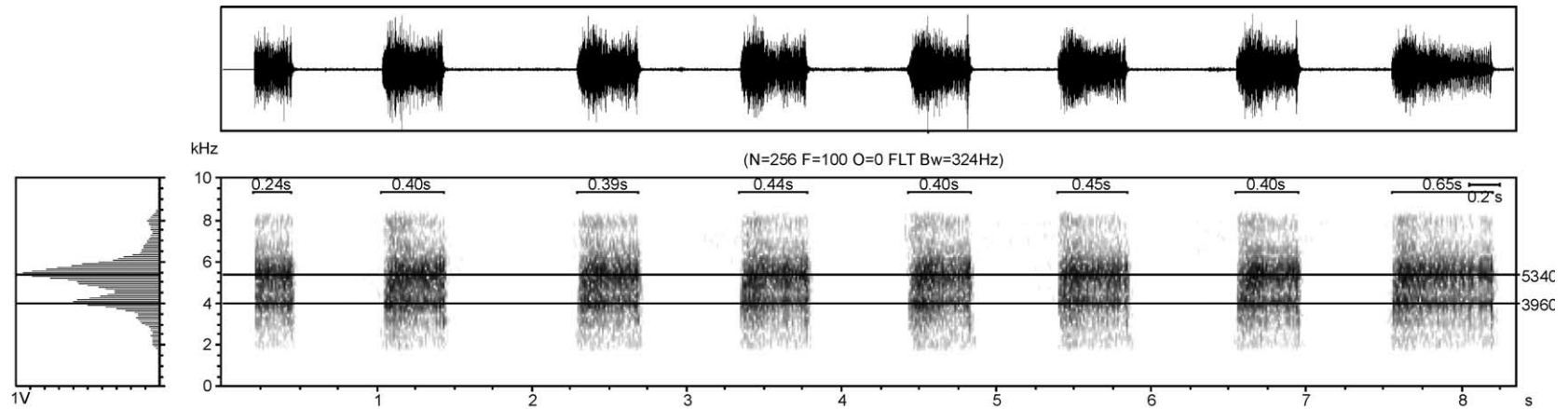
Appendix C

(a) Female guiding call of *Dendrobates variabilis* from Tarapoto, Cordillera Oriental, Peru; lab recording at 24.3 °C. Recorded with a Sony TCM 5000 EV tape recorder and a Sennheiser ME 66-K6 microphone



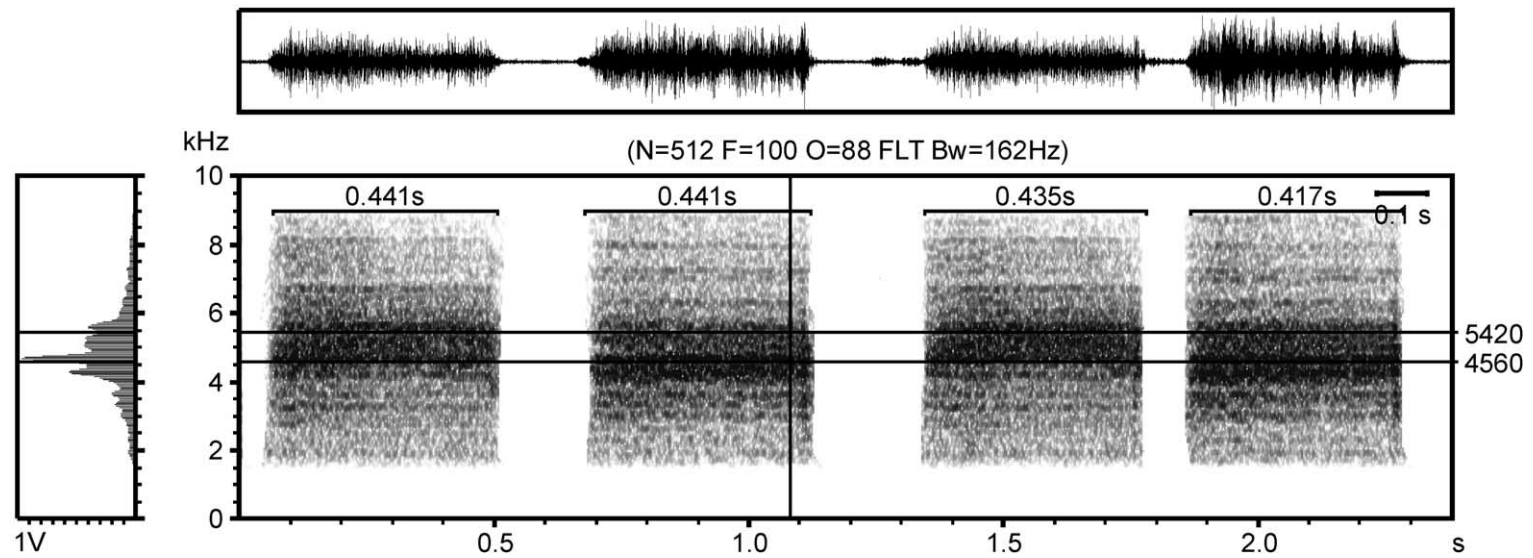
<i>Dendrobates variabilis</i>, SPS , Lab record 24,3°C			
Event	Duration	Interval	Peak freq(mean)
1	0.580	—	4650
2	0.730	1.820	4650
3	0.630	1.720	4470
4	0.750	1.500	4650
5	0.560	1.660	4560
6	0.590	1.420	4560
7	0.540	1.630	4470
8	0.520	1.820	4650
Min	0.520	1.420	4470
Max	0.750	1.820	4650
Mean	0.613	1.653	4583

(b) Female guiding call of *Dendrobates ventrimaculatus* from Bonilla Lowland Forest, Cordillera Oriental, Peru; lab recording at 24.4 °C. Recorded with a Sony TCM 5000 EV tape recorder and a Sennheiser ME 66-K6 microphone



<i>Dendrobates ventrimaculatus</i> , B6-441			
Female Guiding call series, 24,4°C			
Event	Duration	Interval	Peak freq(mean)
1	0.238	—	5250
2	0.394	0.824	5340
3	0.394	1.259	5340
4	0.429	1.050	5340
5	0.400	1.085	5250
6	0.441	0.969	5340
7	0.400	1.149	5250
8	0.644	1.004	5340
Min	0.238	0.824	5250
Max	0.644	1.259	5340
Mean	0.418	1.049	5306

(c) *Dendrobates variabilis* and *Dendrobates ventrimaculatus* in neighbouring cages calling together, 23.8°C. Lower call is *D. variabilis*, higher *D. ventrimaculatus*. *D. variabilis* has more harmonic levels than *D. ventrimaculatus*, but a lower carrier frequency. In the original sound track, the difference is distinctly audible. Recorded with a Sony TCM 5000 EV tape recorder and a Sennheiser ME 66-K6 microphone



References

- Applied Biosystems, Inc. (1995). Autoassembler version 1.4.0.
- Avice, J.C., 2000. Phylogeography: The History and Formation of Species. Harvard University Press, Cambridge, MA.
- Bickham, J.W., Lamb, T., Minx, P., Patton, J.C., 1996. Molecular systematics of the genus *Clemmys* and the intergeneric relationships of emydid turtles. *Herpetologica* 52, 89–97.
- Boulenger, G.A., 1883. On a collection of frogs from Yurimaguas, Huallaga River, northern Peru. *Proc. Zool. Soc. Lond.* 1883, 635–638.
- Broughton, R., Stanley, S., Durrett, R., 2000. Quantification of homoplasy for nucleotide transitions and transversions and a reexamination of assumptions in weighted phylogenetic analysis. *Syst. Biol.* 49, 617–627.
- Brown Jr., K.S., 1982. Historical and ecological factors in the biogeography of aposematic neotropical butterflies. *Am. Zool.* 22, 453–471.
- Caldwell, J.P., Myers, C.W., 1990. A new poison frog from Amazonian Brazil, with further revision of the *quinquevittatus* group of *Dendrobates*. *Am. Mus. Novit.* 21, 1–21.
- Capparella, A., 1988. Genetic variation in Neotropical birds: implications for the speciation process. *Acta XIX Cong. Int. Ornith. (Ottawa 1986)* 2, 1658–1664.
- Chek, A.A., Loughheed, S.C., Bogart, J.P., Boag, P.T., 2001. Perception and history: molecular phylogeny of a diverse group of neotropical frogs, the 20-chromosome *Hyla* (Anura: Hylidae). *Mol. Phyl. Evol.* 8, 370–385.
- Clough, M., Summers, K., 2000. Phylogenetic systematics and biogeography of the poison frogs: evidence from mitochondrial DNA sequences. *Biol. J. Linn. Soc.* 70, 515–540.
- Duellman, W.E., 1982. Quaternary climatic-ecological fluctuations in the lowland tropics: frogs and forests. In: Prance, G.T. (Ed.), *Biological Diversification in the Tropics*. Columbia University Press, New York, pp. 389–402.
- Felsenstein, J., 1985. Confidence limits on phylogenies: an approach using the bootstrap. *Evolution* 39, 783–791.
- Froehlich, J.W., Supriatna, J., Froehlich, P.H., 1991. Morphometric analysis of *Ateles*: systematic and biogeographic implications. *Am. J. Primatol.* 25, 1–22.
- Gascon, C.S., Loughheed, S.C., Bogart, J.P., 1998. Patterns of genetic population differentiation in four species of Amazonian frogs: a test of the Riverine Barrier hypothesis. *Biotropica* 30, 104–119.
- Gascon, C.S., Malcolm, J.R., Patton, J.L., da Silva, M.N.F., Bogart, J.P., Loughheed, S.C., Peres, C.A., Neckel, S., Boag, P.T., 2000. Riverine barriers and the geographic distribution of Amazonian species. *Proc. Natl. Acad. Sci. USA* 97, 13672–13677.
- Goldman, N., Anderson, J.P., Rodrigo, A.G., 2000. Likelihood-based tests of topologies in phylogenetics. *Syst. Biol.* 49, 652–670.
- Haffer, J., 1969. Speciation in Amazonian forest birds. *Science* 165, 131–137.
- Haffer, J., 1990. Geoscientific aspects of allopatric speciation. In: Peters, G., Hutterer, R. (Eds.), *Vertebrates in the Tropics*. Museum A. Koenig, Bonn, Germany, pp. 45–60.
- Haffer, J., 1997. Alternative models of vertebrate speciation in Amazonia: an overview. *Biodivers. Conserv.* 6, 451–476.
- Kimura, M., 1980. A simple method for estimating evolutionary rate of base substitutions through comparative studies of nucleotide sequences. *J. Mol. Evol.* 16, 111–120.
- Kishino, H., Hasegawa, M., 1989. Estimate of the maximum likelihood estimate of the evolutionary tree topologies from DNA sequence data, and the branching order in Hominoidea. *J. Mol. Evol.* 31, 151–160.
- Kjer, K.M., 1995. Use of the rRNA secondary structure in phylogenetic studies to identify homologous positions: an example of alignment and data presentation from the frogs. *Mol. Phyl. Evol.* 4, 314–330.
- Kocher, T.D., Thomas, W.K., Meyer, A., Edwards, S.V., Paabo, S., Villibalanca, F.X., Wilson, A.C., 1989. Dynamics of mitochondrial DNA evolution in animals: amplification and sequencing with conserved primers. *Proc. Natl. Acad. Sci. USA* 86, 6196–6200.
- Loughheed, S.C., Gascon, C., Jones, D.A., Bogart, J.P., Boag, P.T., 1999. Ridges and rivers: a test of competing hypotheses of Amazonian diversification using a dart-poison frog (*Epipedobates femoralis*). *Proc. R. Soc. Lond. B* 266, 1829–1835.
- Lundberg, J.G., Marshall, L.G., Guerrero, J., Horton, B., Malabarba, M.C.S.L., Wesselingh, F., 1998. The stage for neotropical fish diversification: a history of South American rivers. In: Malabarba, M.C.S.L., Reis, R.E., Vari, R.P., Lucena, Z.M., Lucena, C.A.S. (Eds.), *Phylogeny and Classification of Neotropical Fishes*. Edipucrs, Porto Alegre, Brazil, pp. 13–48.
- Lynch, J.D., 1979. The amphibians of the lowland tropical forests. In: Duellman, W.E. (Ed.), *The South American Herpetofauna: its Origin, Evolution, and Dispersal*. University of Kansas Museum of Natural History, Lawrence, Kansas, pp. 189–215.
- Maddison, W.P., Maddison, D.R., 1993. *MacClade 3.03*. Sinauer Associates, Inc., Sunderland, MA.
- Mayr, E., 1942. *Systematics and the Origin of Species*. University of Columbia Press, New York.
- Morales, V.R., 1992. Dos especies nuevas de *Dendrobates* (Anura: Dendrobatidae) para Peru. *Carribb. J. Sci.* 28, 191–199.
- Moritz, C., Dowling, T.E., Brown, W.M., 1987. Evolution of animal mitochondrial DNA: relevance for population biology and systematics. *Ann. Rev. Ecol. Syst.* 18, 269–292.
- Moritz, C., Patton, J.L., Schneider, C.J., Smith, T.B., 2000. Diversification of rainforest faunas: an integrated molecular approach. *Ann. Rev. Ecol. Syst.* 31, 533–563.
- Myers, C.W., 1982. Spotted poison frogs: descriptions of three new *Dendrobates* from Western Amazonia, and resurrection of a lost species from “Chiriqui”. *Am. Mus. Novit.* 2721, 1–23.
- Myers, C.W., 1987. New generic names for some neotropical poison frogs (Dendrobatidae). *Pap. Av. Zool. S. Paulo* 36, 301–306.
- Nores, M., 1999. An alternative hypothesis for the origin of Amazonian bird diversity. *J. Biogeog.* 24, 475–485.
- Ortí, G., Meyer, A., 1997. The radiation of characiform fishes and the limits of resolution of mitochondrial ribosomal DNA sequences. *Syst. Biol.* 46, 75–100.
- Palumbi, S., Martin, A., Romano, S., McMillan, W.O., Stice, L., Grabowski, G., 1991. *The Simple Fools Guide to PCR*, Version 2.0. University of Hawaii, Honolulu, Hawaii.
- Patton, J.L., daSilva, M.N.F., Malcolm, J.R., 1994. Gene genealogy and differentiation among arboreal spiny rats (Rodentia: Echimyidae) of the Amazon basin: a test of the riverine barrier hypothesis. *Evolution* 48, 1314–1323.
- Patton, J.L., da Silva, M.N.F., 1998. Rivers, refuges and ridges: the geography of speciation of Amazonian mammals. In: Howard, D.J., Berlocher, S.H. (Eds.), *Endless Forms: Species and Speciation*. Oxford University Press, New York, pp. 202–212.
- Posada, D., Crandall, K., 1998. Modeltest: testing the model of DNA substitution. *Bioinformatics* 14, 817–818.
- Prance, G.T. (Ed.), 1982. *Biological Diversification in the Tropics*. Columbia University Press, New York.
- Prance, G.T., 1973. Phytogeographical support for the theory of forest refuges in the Amazon Basin, based on evidence from distribution patterns in Caryocaraceae, Chrysobalanaceae, Dichapetalaceae and Lecythidaceae. *Acta Amazon.* 3, 5–28.
- Räsänen, M.E., Salo, J.S., Kalliola, R.J., 1987. Fluvial perturbation in the Western Amazon basin: regulation by long-term sub-Andean Tectonics. *Science* 238, 1398–1401.
- Räsänen, M.E., Salo, J.S., Jungner, H., Pittman, L.R., 1990. Evolution of the western Amazon lowland relief: impact of Andean foreland dynamics. *Terra Nova Res.*, 320–332.

- Räsänen, M.E., Salo, J.S., Jungner, H., 1991. Holocene floodplain lake sediments in the Amazon: ^{14}C dating and Paleoecological use. *Quart. Sci. Rev.* 10, 363–372.
- Räsänen, M.E., Neller, R., Salo, J., Jungner, H., 1992. Recent and ancient fluvial deposition systems in the Amazonian foreland basin, Peru. *Geol. Mag.* 129, 293–306.
- Räsänen, M.E., Linna, A.M., Santos, J.C.R., Negri, F.R., 1995. Late Miocene tidal deposits in the Amazonian foreland basin. *Science* 269, 386–389.
- Rodríguez, F., Oliver, J.L., Marín, A., Medina, J.R., 1990. The general stochastic model of nucleotide substitution. *J. Theor. Biol.* 142, 485–501.
- Ruokolainen, K., Linna, A., Tuomisto, H., 1997. Use of Melastomataceae and pteridophytes for revealing phylogeographical patterns in Amazonian rain forests. *J. Trop. Ecol.* 13, 243–256.
- Schluter, D., 1998. Ecological causes of speciation. In: Howard, D.J., Berlocher, S.H. (Eds.), *Endless Forms: Species and Speciation*. Oxford University Press, Oxford, pp. 114–129.
- Schulte, R., 1986. Eine neue *Dendrobates* – ART aus OSTPERU (Amphibia: Salienta: Dendrobatidae). *Sauria* 8, 11–20.
- Schulte, R., 1999. Die Pfeilgiftfrösche Vol. II. Artenteil. INIBICO, Waiblingen, Peru.
- Shreve, B., 1935. On a new teiid and Amphibia from Panama, Ecuador, and Paraguay. *Occas. Pap. Boston Soc. Nat. Hist.* 8, 209–218.
- Sick, H., 1967. Rios e enchentes na Amazonia como obstáculo para a avifauna. *Atlas Simposia Bioto Amazônica (Zool.)* 5, 495–520.
- Silverstone, P.A., 1975. A revision of the poison-arrow frogs of the genus *Dendrobates* Wagler. *Nat. Hist. Mus. L.A. Co. Sci. Bull.* 21, 1–51.
- Steindachner, F., 1864. *Batrachologische Mittheilungen*. *Verh. K.K. Zool.-Bot. Ges., Vienna* 14, 239–288 + pls 9–17.
- Summers, K., Weigt, L.A., Boag, P., Bermingham, E., 1999. The evolution of parental care in poison frogs of the genus *Dendrobates*: evidence from mitochondrial DNA sequences. *Herpetologica* 55, 254–270.
- Swofford, D.L., 1999. *Phylogenetic Analysis Using Parsimony (PAUP): Version 4.0*. Smithsonian Natural History Museum, Washington.
- Symula, R., Schulte, R., Summers, K., 2001. Molecular phylogenetic evidence for a mimetic radiation in Peruvian poison frogs supports Müllerian mimicry hypothesis. *Proc. R. Soc. Lond. B* 268, 2415–2421.
- Taylor, P.L., 1990. *Gene Jockey sequence processor: Version 1.20*. Biosoft, Cambridge.
- Thompson, J.D., Gibson, T.J., Plewniak, F., Jeanmougin, F., Higgins, D.G., 1997. The ClustalX windows interface: flexible strategies for multiple sequence alignment aided by quality analysis tools. *Nucl. Acids Res.* 24, 4876–4882.
- Tuomisto, H., Ruokolainen, K., Kalliola, R., Linna, A., Danjoy, W., Rodriguez, Z., 1995. Dissecting Amazonia biodiversity. *Science* 269, 63–66.
- Vanzolini, P.E., 1970. *Zoologia sistématica, geografia e a origem das espécies*. *Inst. Geog. S. Paulo Teses e Monog.* 3, 1–56.
- Vences, M., Kosuch, J., Lötters, S., Widmer, A., Jungfer, K.H., Köhler, J., Veith, M., 2000. Phylogeny and classification of poison frogs (Amphibia: Dendrobatidae), based on mitochondrial 16S and 12S ribosomal RNA gene sequences. *Mol. Phyl. Evol.* 15, 34–40.
- Wallace, A.R., 1853. *A Narrative of Travels on the Amazon and Rio Negro*. Reeve, London.
- Williams, P.L., Fitch, W.M., 1990. Phylogeny determination using a dynamically weighted parsimony method. *Meth. Enzymol.* 183, 615–626.
- Yang, Z., 1996. Among site variation and its impact on phylogenetic analyses. *Trends Ecol. Evol.* 11, 367–371.
- Zimmerman, H., Zimmerman, E., 1988. Ethotaxonomie und zoogeographische ARTENGRUPPENBILDUNG bei PFEILGIFTFRÖSCHEN (Anura: Dendrobatidae). *Salamandra* 24, 125–160.